

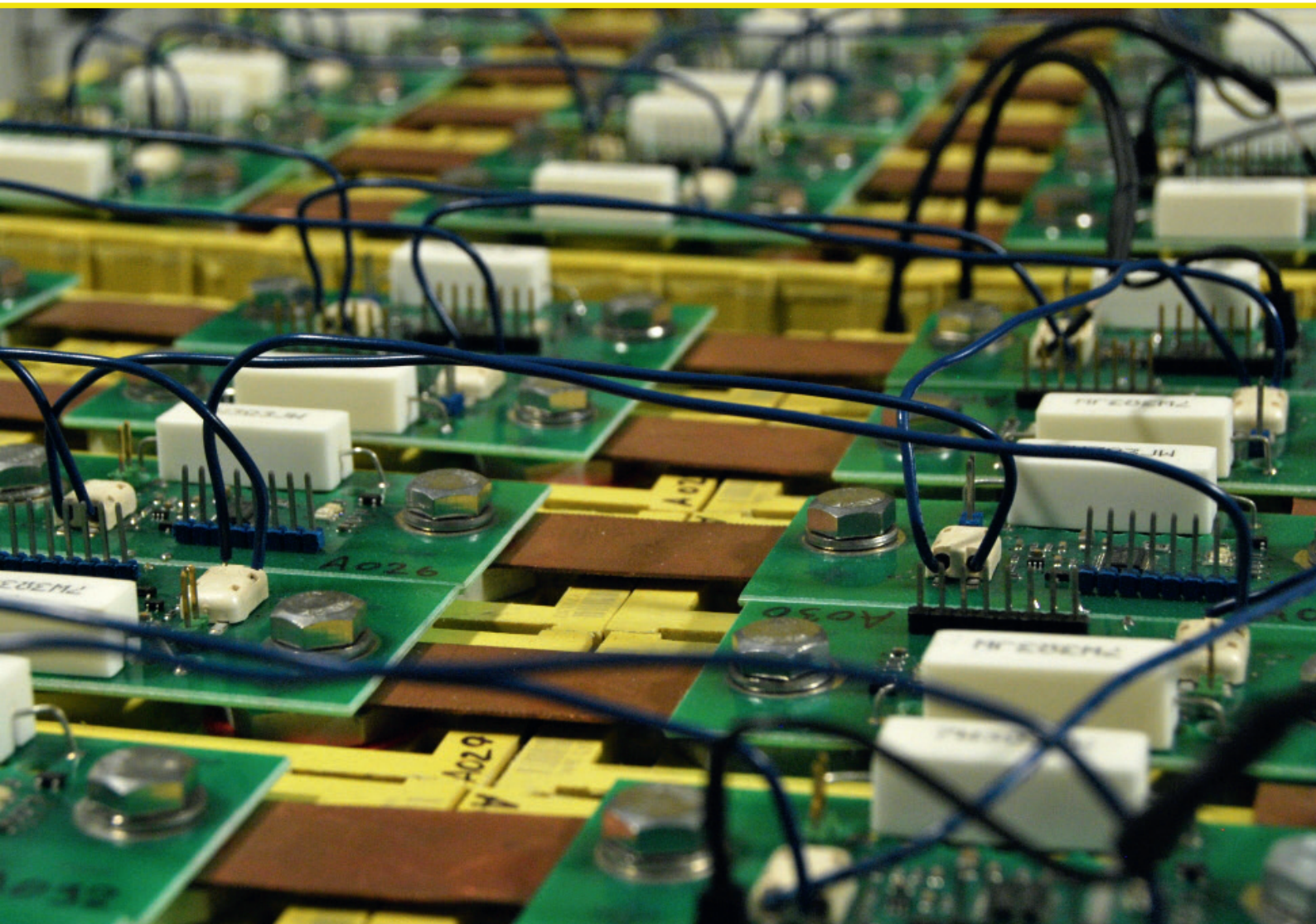


RIGA TECHNICAL
UNIVERSITY

Kristaps Vītols

**RESEARCH AND DEVELOPMENT OF BATTERY
PACKS AND THEIR BALANCING METHODS
FOR PERSONAL MOBILITY VEHICLES**

Summary of the Doctoral Thesis



RTU Press
Riga 2022

RIGA TECHNICAL UNIVERSITY
Faculty of Electrical and Environmental Engineering
Institute of Industrial Electronics and Electrical Engineering

Kristaps Vītols

Doctoral Student of Study Programme “Computerised Control of Electrical Technologies”

**RESEARCH AND DEVELOPMENT OF
BATTERY PACKS AND THEIR BALANCING
METHODS FOR PERSONAL MOBILITY
VEHICLES**

Summary of the Doctoral Thesis

Scientific supervisor
Professor Dr. sc. ing.
IĻJA GALKINS

RTU Press
Riga 2022

Vītols K. Research and Development of Battery Packs and their Balancing Methods for Personal Mobility Vehicles. Summary of the Doctoral Thesis. – Riga: RTU Press, 2022. – 33 p.

Published in accordance with the decision of the Promotion Council “RTU P-14” of 8 February 2022, Minutes No. 04030-9.12.1/2.

To my family

Cover picture by Aleksandrs Suzdaļenko.

This work has been supported by the European Social Fund within project “Support for the implementation of doctoral studies at Riga Technical University” and by the European Social Fund project “Development of the Academic Personnel of Riga Technical University” No. 8.2.2.0/18/A/017.



<https://doi.org/10.7250/9789934227660>
ISBN 978-9934-22-766-0 (pdf)

DOCTORAL THESIS PROPOSED TO RIGA TECHNICAL UNIVERSITY FOR THE PROMOTION TO THE SCIENTIFIC DEGREE OF DOCTOR OF SCIENCE

To be granted the scientific degree of Doctor of Science (Ph. D.), the present Doctoral Thesis has been submitted for the defence at the open meeting of RTU Promotion Council on 27 May 2022 at 14.00 in the Conference Hall of RTU Conference and Sports Centre “Ronīši”, Klapkalnciems, Engure County.

OFFICIAL REVIEWERS

Associate Professor Dr. sc. ing. Jānis Zaķis
Riga Technical University

Professor Ph. D. Enrique Romero-Cadaval
University of Extremadura, Spain

Senior Researcher Ph. D. Andrei Blinov
Tallinn University of Technology, Estonia

DECLARATION OF ACADEMIC INTEGRITY

I hereby declare that the Doctoral Thesis submitted for the review to Riga Technical University for the promotion to the scientific degree of Doctor of Science (Ph. D.) is my own. I confirm that this Doctoral Thesis had not been submitted to any other university for the promotion to a scientific degree.

Kristaps Vītols(Signature)

Date:

The Doctoral Thesis has been written in English. It consists of Introduction, 7 chapters, Conclusion, 86 figures, 7 tables, 5 appendices; the total number of pages is 165, including appendices. The Bibliography contains 220 titles.

Contents

INTRODUCTION.....	5
MAIN HYPOTHESIS AND OBJECTIVES.....	5
Hypothesis.....	5
Objectives.....	5
Means and methods of research	5
Scientific novelties	6
Practical novelties	6
Practical application of research results	6
Dissemination of research results.....	7
1. ANALYSIS OF ELECTRIC VEHICLE BATTERIES.....	8
2. LITHIUM-ION BATTERY TECHNOLOGY INVESTIGATION	10
3. ANALYSIS OF BATTERY MANAGEMENT SYSTEMS	12
4. INVESTIGATION OF INDIVIDUAL CELL TESTING METHODS	18
5. THE DEVELOPMENT OF A BATTERY CONFIGURATION FOR A PMV	21
6. CELL BALANCING SYSTEM DEVELOPMENT AND VERIFICATION.....	23
7. DEVELOPMENT OF ADVANCED CELL BALANCING.....	26
CONCLUSIONS	29
REFERENCES.....	30

INTRODUCTION

The recent advances in the commercial electric vehicle (EV) sector by the major automotive industry members are quite obvious. Steadily more and more electric vehicles are appearing on the market and on the roads of Latvia as well [1]. Conventional internal combustion engines are shifting toward electric technologies by introducing hybrid technologies where additional electric motors with their battery packs are added to the vehicle to improve the performance. The major driving force behind this is the goal to achieve sustainable economy and environmental neutrality – to stop the climate change by reducing greenhouse gas emissions [2], [3].

The electric vehicle portfolio is additionally expanded by electric personal mobility vehicles (PMV). The visibility and availability of PMVs is greatly increased by companies providing short- or long-term leasing of e-scooters and e-bicycles in many countries.

In Latvia e-mobility is developing as well. Riga Technical University is shifting towards fully electric vehicle fleet: more than a dozen EVs have been purchased and are successfully utilized. A local rallycross vehicle designer and manufacturer *OSC*, led by engineer and designer Andris Dambis, has been developing racing electric vehicles and electric public transport minibuses [4]. Another notable example is the Blue Shock Race team, which is developing high performance electric race karts [5].

The key to all this progress is the advent of modern lithium-ion battery technology. A battery management system (BMS) is required for every Li-ion battery pack to keep its operational variables within set limits. A disconnect switch can be used in the simplest BMS when a battery is approaching a critical state. In larger multi-cell batteries, an additional circuit is used to keep cells equally balanced to optimize the performance of the whole pack. There is a wide variety of such battery balancing circuits or methods in research literature.

The initial motivation for this Thesis is to design a battery pack for an ongoing electric kart for an educational project – a personal mobility vehicle in a broader sense.

MAIN HYPOTHESIS AND OBJECTIVES

Hypothesis

The balancing performance of a battery management system can be improved by combining two different balancing methods into a two-layer balancing solution.

Objectives

1. To analyse the present electric vehicle battery systems.
2. To investigate lithium-ion battery technology and analyse the present battery balancing methods.
3. To perform investigative testing of lithium-ion cells.
4. To utilize the obtained knowledge to design a battery pack for a small electric vehicle.
5. To develop a custom two-layer balancing system.

Means and methods of research

MS Excel has been extensively used for calculations and data processing, especially for statistical analysis. *Matlab* was used for data processing, visualization, and measurement

process automation – instrumentation control scripts were designed and executed. *HxD hex editor* software was used to obtain raw data from memory cards, which were used for cell data logging. *LTspice* has been used for preliminary simulations of various parts of designed circuits.

During the development, testing and experimental verification, a variety of laboratory equipment was used in different configurations. The list of used equipment includes various power supplies, oscilloscopes with assortment of probes, a thermal imaging camera, a battery impedance meter, electronic loads, precision power analyser and several multimeters.

A few models of *MSP430* family microcontrollers were used throughout this project. Both *IAR Embedded Workbench* (mostly in assembly language) and *Code Composer Studio* (mostly in C language) were used to program and debug microcontrollers. *Orcad Capture, Layout* and *PCB editor* was used for most PCB design. Occasionally, *Altium designer* was used as well. Experimental PCBs were manufactured in-house using PCB milling, while proven board manufacturing was outsourced.

Scientific novelties

1. Switched resistor and multi-secondary winding transformer balancing methods have been combined for the first time to produce a two-layer balancing solution.
2. A novel battery balancing categorization is proposed, which groups the existing methods into dissipative methods, selective charging/discharging methods, and charge transfer methods.
3. A statistical analysis of unused cell parameters has been presented, which indicates small differences in parameters, which, in turn, justify the use of switched resistor balancing.

Practical novelties

1. An analysis process of battery voltage and configuration selection process has been provided for a power assist wheelchair.
2. A fully modular switched resistor balancing board with a daisy-chain data exchange has been developed.
3. Procedure and hardware have been developed to calibrate both cell voltage and temperature measurements of the developed balancing boards.

Practical application of research results

1. The developed switched resistor balancing board (version 2) has been implemented in a 20-cell battery pack for an electric kart.
2. The developed switched resistor balancing solution (version 3) has been implemented in a 144-cell battery pack for a DC microgrid battery energy storage system.
3. The provided battery design process has been used to develop a battery pack for a power-assisted wheelchair. The pack prototype has been equipped with a battery management system and case/housing combo, which permits easy battery pack replacement.

Dissemination of research results

The author has a total of 33 publications and a chapter in a book. The following 13 publications are presented in the Doctoral Thesis:

1. R. Zemnieks and **K. Vitols**, “Automation of Battery Impedance Measurement Using Matlab,” in *2020 IEEE 61st Annual International Scientific Conference on Power and Electrical Engineering of Riga Technical University, RTUCON 2020 – Proceedings*, 2020.
2. **K. Vitols** and A. Podgornovs, “Impact of battery cell configuration to powered wheelchair drive efficiency,” *Arch. Electr. Eng.*, vol. 69, no. 1, pp. 203–213, 2020.
3. **K. Vitols** and E. Grinfogels, “Battery Batch Impedance Analysis for Pack Design,” in *2019 IEEE 7th IEEE Workshop on Advances in Information, Electronic and Electrical Engineering (AIEEE)*, 2019, pp. 1–5.
4. **K. Vitols**, E. Grinfogels, and D. Nikonorovs, “Cell Capacity Dispersion Analysis Based Battery Pack Design,” in *2018 6th IEEE Workshop on Advances in Information, Electronic and Electrical Engineering (AIEEE)*, 2018, no. 1, pp. 1–5.
5. **K. Vitols** and E. Poiss, “Development of Electric Scooter Battery Pack Management System,” in *2018 IEEE 59th International Scientific Conference on Power and Electrical Engineering of Riga Technical University (RTUCON)*, 2018, pp. 1–5.
6. **K. Vitols** and A. Podgornovs, “Concept of cost-effective power-assist wheelchair’s electrical subsystem,” in *2017 5th IEEE Workshop on Advances in Information, Electronic and Electrical Engineering (AIEEE)*, 2017, pp. 1–4.
7. **K. Vitols**, “Efficiency of LiFePO₄ battery and charger with a mixed two level balancing,” in *2016 57th International Scientific Conference on Power and Electrical Engineering of Riga Technical University (RTUCON)*, 2016, pp. 1–4.
8. **K. Vitols**, “Efficiency of LiFePO₄ Battery and Charger with Passive Balancing,” in *AIEEE 2015*, 2015.
9. **K. Vitols**, “Lithium ion battery parameter evaluation for battery management system,” in *2015 56th International Scientific Conference on Power and Electrical Engineering of Riga Technical University (RTUCON)*, 2015, pp. 1–4.
10. **K. Vitols**, “Design considerations of a battery pack - DC grid interface converter,” in *2015 IEEE 5th International Conference on Power Engineering, Energy and Electrical Drives (POWERENG)*, 2015, vol. 2015-Septe, pp. 476–479.
11. **K. Vitols** and I. Galkin, “Evaluation of cell balancing solution with a custom energy measurement device design,” in *2014 55th International Scientific Conference on Power and Electrical Engineering of Riga Technical University, RTUCON 2014*, 2014.
12. **K. Vitols**, “Redesign of passive balancing battery management system to active balancing with integrated charger converter,” in *2014 14th Biennial Baltic Electronic Conference (BEC)*, 2014, pp. 241–244.
13. **K. Vitols**, “Design of an embedded battery management system with passive balancing,” in *2014 6th European Embedded Design in Education and Research Conference (EDERC)*, 2014, pp. 142–146.

1. ANALYSIS OF ELECTRIC VEHICLE BATTERIES

Light-duty electric vehicles were reviewed to obtain data regarding the battery construction and balancing performance. *Volkswagen e-up!* initially in year 2012 had only an 18.7 kWh battery pack, which provided 130 km of range. The current version of *e-up!* uses a 32.3 kWh battery, which is capable of up to 260 km of driving range [6]. *Nissan Leaf* had a 24/30 kWh Li-ion battery, while the new version is equipped with a 40 kWh LIB, which is made of 192 NMC pouch cells [7]. BMS PCBA images from amateur teardowns indicate that custom labeled ASICs are used for cell monitoring and balancing [8]. A switched resistor balancing is used with a single 430 Ω shunting resistor per cell. Given that cells are arranged in 96S2P configuration, it can be calculated that each cell pair has approximately 116 Ah capacity – the shunting resistor provides less than 10 mA of current for this cell pair. 0.000084 A/Ah current is selected to do the balancing. *BMW i3* battery is made of high-capacity prismatic NMC Li-ion cells at 22 kWh, 33 kWh and 42.2 kWh capacities [9]. *LTC6801* independent multicell battery stack fault monitor IC and *LTC6802-2* multicell addressable battery stack monitor IC from *Linear Technologies* are used to monitor voltages and temperatures of the cells and perform switched resistor balancing [10]. 2512-size 56 Ω surface mount resistor is used to balance each cell with 75 mA or 0.00125–0.000625 A/Ah. *Tesla S* uses 18650-size battery cells from *Panasonic*, presumably Li-ion NCA type. According to amateur teardowns, a nominal 85 kWh battery pack is made using the 96S74P cell configuration producing approximately 400 V when fully charged [11]. The 74 cells in parallel are referred to as the brick. Six bricks are series connected to make a module, and 16 modules are further series connected to make the battery pack. Each module is equipped with a local battery management board, which is built around the *BQ76PL536A* battery monitor and secondary protection IC [12]. *BQ76PL536A* controls an external transistor to connect four 1206 size 158 Ω resistors to the required cell. It can be calculated that 106 mA balancing current is used to balance a 244 Ah “cell” (brick made of 76 cells), hence just 0.00043 A/Ah balancing current proportion is used.

In general, light-duty EVs are mostly using Li-ion batteries with NMC chemistry, except for *Tesla*, which uses Li-ion NCA chemistry [13]. Switched resistor balancing is used to equalize cells with current ranging from just 84 μ A to 1.25 mA per Ah of a cell.

A variety of different “smaller-than-typical-car” personal mobility vehicles exist on the market. Among two wheeled vehicles, electric bicycles and scooters with 36V Li-ion battery are the most popular. Nominal voltage range is much broader, ranging from 12 V up to 72 V. The typical voltages are 24 V, 36 V and 43 V [14]. While information about cells is not available from most OEMs, in some cases it is indicated that the battery is made of 18650-sized NMC cells. Online amateur teardowns indicate that 18650-size is predominantly popular [15]. Alternatively, 26650- and 20700/21700-sizes and LFP chemistry is used. The energy content of reviewed battery packs varied from 200 Wh to 750 Wh with distinctive groups at 400 Wh and 500 Wh. Market analysis of electric seatless kick scooters shows a wide variety of models with different capabilities. Major online store *Banggood* offers 101 electric scooters, while the offer of *Amazon* is not as categorized and yields around 240 electric articles, which include proper electric scooters, their parts, unicycles, self-balance boards, hoverboards, hovershoes, three wheeled scooters, onewheels and even underwater electric scooters and other personal

electric transport vehicles. The offer of 16 dedicated online stores was analyzed to obtain specific information regarding a total of 238 electric kick scooter models and their clones. The slowest scooters are equipped with a single 90–200 W chain drive motor. Series connected sealed lead acid batteries can be found among these models to supply 12 V to 24 V at capacities in 100–200 Wh range. In more expensive models, state-of-art brushless hub motors and 36 V Li-ion batteries can be found with capacities as high as 200 Wh. The 25 km/h group is mostly equipped with front or rear hub motor rated at 250–350 W. Batteries are composed of 18650-sized Li-ion cells at pack capacities ranging from 150 Wh to 300 Wh at 36 V. High speed scooters use 18650-sized cells at higher total capacities and voltages. The max speed can be as high as 120 km/h ,while a 35–160 km range is achieved using 48–72 V battery packs at 300–3000 Wh capacities. Model distribution vs battery capacity is shown in Fig. 1.1.

To summarize and conclude, it is obvious that battery EVs of all kinds use lithium-ion batteries. Majority of batteries are of NMC and NCA chemistries, while in some specific cases LFP and even LTO chemistries are used. One of the objectives of this chapter was to provide insight in cell balancing methods used in various EVs. Unfortunately, vehicle manufacturers do not provide information about their BMS. The only usable information was amateur and professional EV battery teardowns as well as spare part images. From the available information it was concluded that the switched resistor balancing method is used predominantly. Even in large battery packs (20–100 kWh) small surface mount resistors are used to dissipate excessive energy at a currents less than 1 mA. This brings up questions: are cells produced of such qualities that mismatch is miniscule; has battery pack design evolved so far that uniform conditions exist for all cells; is cell energy mismatch a real problem; are there requirements for higher rate/shorter time balancing?

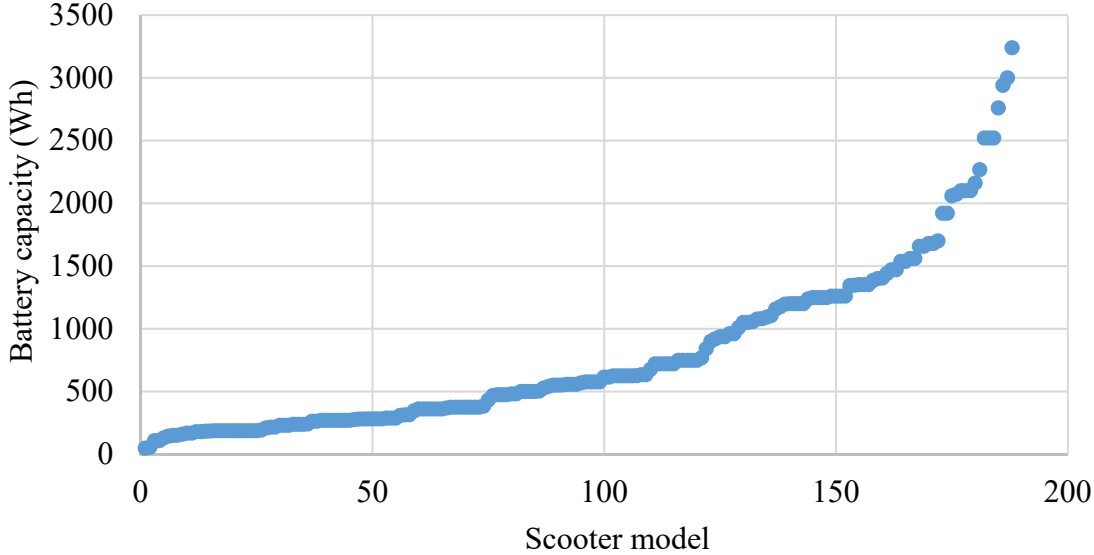


Fig. 1.1. Battery capacity distribution of reviewed electric seatless kick scooters.

2. LITHIUM-ION BATTERY TECHNOLOGY INVESTIGATION

During the last decades lithium-ion battery technology has evolved quickly, overtaking significant part of the market, and the total worth of related technologies is expected to grow in the future [16]. It is estimated that total LIB market is in the 30-billion-euro range, and it is expected to increase fourfold in this decade [16]. Over the 30-year period of commercialization, LIBs have become a dominant battery technology with room for improvement.

There are six common Li-ion chemistries, which differ according to the materials used in both electrodes. The widest variety is for the positive electrode (cathode), which can have five compositions: LCO, LMO, NMC, NCA, and LFP. Anode usually is composed of carbon, while an alternative is LTO. NMC is a popular type for EVs. It used to have a 1:1:1 ratio between nickel, manganese and cobalt, hence an extended name was NMC111. Then, chemistry was improved to reduce the cobalt content, and a new NMC622 type modification was introduced. It is expected that NMC811 material will be available and become mainstream in near future. The key difference between these variations is the increase in gravimetric energy density.

In case of LIBs, full discharge is to be avoided to maximize the battery lifespan. The depth of discharge (DoD) can be calculated using (2.1):

$$DoD = \frac{I_{DCH} \cdot t_{DCH}}{C_{nom}} \cdot 100\%, \quad (2.1)$$

where

DoD – discharged capacity, %;

I_{DCH} – discharge current, A;

t_{DCH} – discharge time, h;

C_{nom} – nominal capacity, Ah.

Often the state of charge (SoC) is used as an inverse of DoD. The discharge rate affects the voltage of the cell – at high rates the voltage will drop more, in some cases it is beneficial to decrease the cut-off voltage to achieve a desired end DoD. In most LIBs the discharge is linear with a drop at the final stage of discharge (90–100 % DoD) when discharged at low rate. However, as the rate is increased, the drop at high DoD becomes flatter, while the voltage drops faster at the opposite end of the curve at low DoD. The discharge performance is affected by the temperature of the cell. For most Li-ion types the available capacity rapidly decreases at low temperature (below $-15\text{ }^{\circ}\text{C}$).

NMC can be rated at 3.6 V to 3.7 V depending on the exact materials and proportions of the cathode. The discharge cut-off varies from 2.7 V to 3 V with 2.5 V as the absolute minimum. NMC is considered to be the leading LIB chemistry with the ability to produce cells with both high energy and power at good cycle life. Gravimetric energy density is more than 200 Wh/kg, and discharge rates up to 2C are achievable. More than 60 % of all LIBs are NMC, and adoption in EVs is more than 50 %.

NCA has 3.6 V nominal voltage and cut-off at 2.5 V. This type is regarded as high energy with good power capability and long life, additionally EV manufacturer *Tesla* together with battery manufacturer *Panasonic* has proven that battery packs with the price less than 200 € per kWh can be manufactured using cylindrical NCA cells [17].

The nominal voltage of an LFP cell is 3.2 V, while the cut-off varies from 2.0 V to 2.5 V. The discharge curve is very flat at rapid voltage curves at both ends. Despite the low cost of materials, LFP cells are expensive because of low gravimetric energy density. The advantages are high power, high safety and long life under specific discharge conditions. Safety includes chemical and thermal stability as well as some tolerance to overcharge and short circuit.

The CCCV charging method is used to charge LIBs. There are two main charging phases: the faster constant-current phase and the slower constant-voltage phase as shown in Fig. 2.1. If a battery is deeply discharged, then a pre-charge phase should be introduced before the full current CC phase [18].

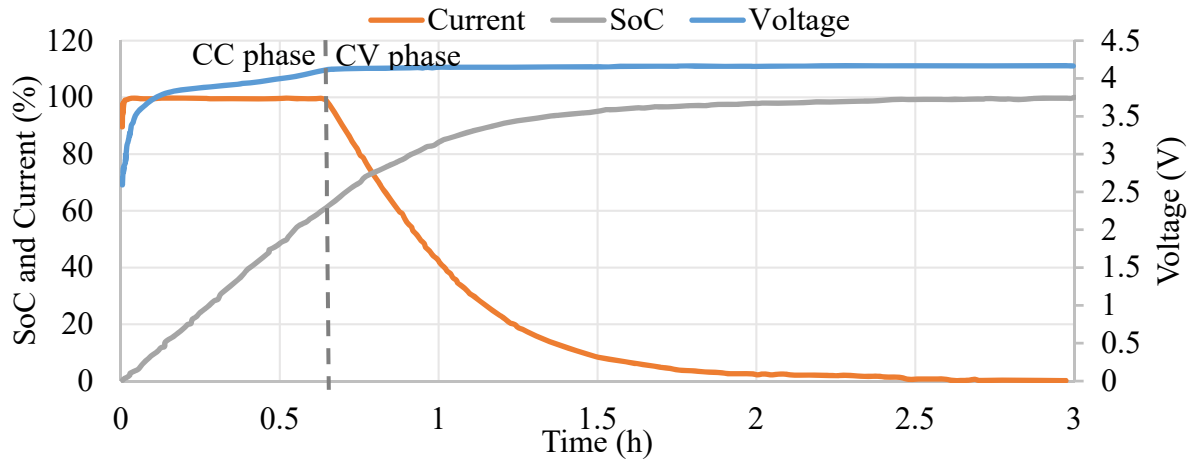


Fig. 2.1. Charging curves of an NMC Li-ion cell. Current is expressed in percentage, where 100 % represent 1C rate.

Most of the charge to the battery is delivered during the CC charging phase. The standard charging rate commonly is 0.5C, which results in approximately 2 to 2.5 hour 0–100 % battery charging (including CV phase). Faster charging can be achieved by using 1C or even 2C rates. In standard charging, most time of charging is spent in the CC phase, when battery is charged to 80–90 % SoC. The CC phase is terminated when the charging voltage level is reached and the charging transitions to CV phase during which the remaining charge is delivered to the battery. Charging during the CV phase happens much slower due to ever decreasing current. When high rate is used in CC phase, the charging voltage limit is reached much faster due to the cell heating and resistive drop [19]. For LCO, LMO, NMC, and NCA chemistries, the charging voltage is 4.2 V. Lower charging voltage naturally results in lower max SoC, hence it is an easy method to decrease the used capacity range. The decreased used capacity (never fully charged, never fully discharged) increases the cycle life. Additionally, keeping a Li-ion cell at its maximum voltage stresses the internal structure, which leads to overall degradation. Lowering the max voltage reduces this internal chemical stress and promotes longer calendar life [20]. Cell balancing is required for multi-cell batteries to reach their max SoC level. Differences among cells lead to long balancing, which can be shortened using the higher performance balancing method. Alternatively, a battery pack can be made using similar (selected) cells, and uniform conditions can be provided to promote even ageing of individual elements.

3. ANALYSIS OF BATTERY MANAGEMENT SYSTEMS

Over the years many different methods to balance the cell voltages or states of charge have been proposed. These methods are categorized into two groups: passive and active [21], [22], [23], [24]. In some articles passive balancing methods are the ones that dissipate excess energy as heat. A traditional passive balancing method is to use a resistor in parallel with each cell to perform balancing. Active balancing methods are intended to remove charge from the higher SoC cells and transfer it to the cells with lower SoC. A circuit with controllable switches and capacitors or inductors is used to transfer energy between cells. In some literature active balancing includes switched resistor balancing – probably because controllable switches are used to connect or disconnect resistors. A direct replacement would be dissipative and non-dissipative balancing. Here it is proposed to further split the non-dissipative group in selective charge/discharge methods and charge transfer methods, as shown in Fig. 3.1.

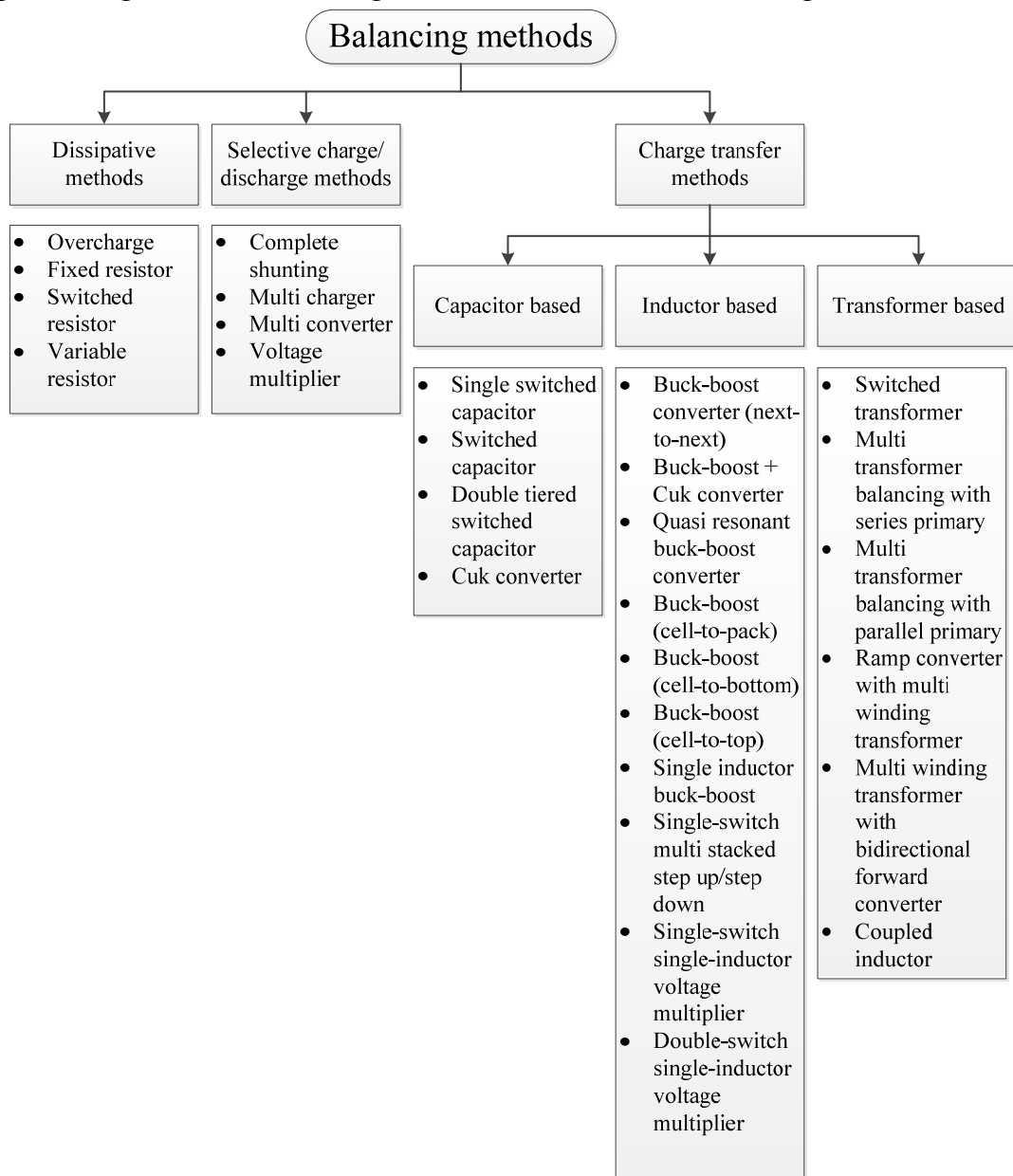


Fig. 3.1. Categories of balancing methods.

The dissipative methods branch is devoted to methods that convert any excessive charge to heat by using resistance of electronic elements or by applying overcharge. Selective charge/discharge group corresponds to auxiliary charger and complete shunting methods while the charge transfer methods incorporates capacitive shuttling and transformer/inductor converter-based methods.

The most commonly used balancing method is switched resistor balancing, which is referred to as bypass resistive shunting, resistive current shunting, charge shunting and dissipative resistor shunting as well. The basic balancing operation is removing the excess charge from the target cell through a resistive element until the charge matches those of the lower cells of the pack or a reference state of charge (Fig. 3.2).

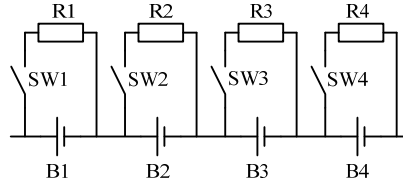


Fig. 3.2. Switched resistor balancing topology.

This type of dissipative balancing with switched shunting resistor is a common balancing method because of its reliability and simplicity [22], [21], [23], [25]. The switched resistor balancing can be designed to operate without a master controller. In such a case each cell is equipped with the same circuit that can measure the parameters of the particular cell and connect the resistor if necessary. However, without a central master module there is no data exchange and overall parameter measurement, which can provide information of battery pack parameters, improve charging process, and improve the balancing process itself.

Switched resistor balancing can be used for both top and bottom balancing. While both types of balancing could be used, the top balancing is traditionally more preferred. In this mode the charging current I_{cell} of each cell can be determined using (3.1), where I_{chg} is the total charging current, V_{cell} is voltage of the cell, R_{bal} is the resistance of the balancing resistor, and R_{on} is the resistance of the switch, which can be similar to R_{bal} . Part of the charging current is diverted to balancing resistor.

$$I_{cell} = I_{chg} - \frac{V_{cell}}{R_{bal} + R_{on}} \quad (3.1)$$

The losses of top balanced switched resistor balancing method can be analysed analytically. When charging the pack, balancing power loss P_{loss} is zero, while no balancing resistor is activated – this amounts for most of time of the charging procedure if cells are equal and closely balanced. During charging, once the first cell reaches full voltage/balancing voltage (V_{bal}), its balancing resistor is activated and charging current is decreased to match the balancing current (an ideal case): $I_{chg} = I_{bal}$.

As a result, the SoC of given cell does not change, while balancing losses appear according to (3.2):

$$P_{cell_loss} = V_{bal} \cdot I_{bal} \quad (3.2)$$

Gradually, more cells reach balancing voltage and add to the total power loss, which can be calculated using (3.3). Eventually, $n - 1$ cells are full and just one cell is being charged – P_{loss} is at max value and can be calculated using (3.4). The charging current is reduced to zero (charging is stopped) once the last cell reaches full voltage, hence P_{loss} becomes zero as well.

$$P_{loss} = \sum_{i=1}^{nbal} P_{cell_loss_i} \quad (3.3)$$

$$P_{loss_max} = (n - 1) \cdot V_{bal} \cdot I_{bal} \quad (3.4)$$

The balancing power loss is a discrete function as the power loss gradually increases in steps from zero to its max value when $n - 1$ cells are full/being balanced. The duration of each step is related to cells SoC mismatch during charging operation.

The total energy loss during the balancing operation is a more useful variable, as it can be easily compared to total energy loss of other balancing methods. Generally, balancing energy loss E_{loss} is an integral of balancing power loss (3.5):

$$E_{loss} = \int_0^{full} P_{loss}(t) dt, \quad (3.5)$$

where

- E_{loss} – total balancing energy loss, Wh;
- $P_{loss}(t)$ – balancing power loss function, W;
- $full$ – time at which balancing is stopped, s.

The integration interval is from the beginning of balancing operation to the end when the last cell reaches its full voltage. As the $P_{loss}(t)$ is a discrete function, then E_{loss} can be expressed as a sum of individual P_{loss} levels (3.6):

$$E_{loss} = \sum_{x=1}^{n-1} (x V_{bal} (\Delta C_{x+1} - \Delta C_x)), \quad (3.6)$$

where

- E_{loss} – total balancing energy loss, Wh;
- n – total number of cells;
- V_{bal} – balancing voltage, V;
- ΔC – capacity difference, Ah.

ΔC is specific to every cell – it shows the relative difference in capacity in respect to the previous cell and the one which is being balanced. For the first cell $\Delta C_1 = 0$, and each next ΔC_x value can be calculated as a difference between the previous C_{x-1} and given cell's C_x value. If the ΔC value span and distribution is narrow, then the resulting E_{loss} will be small. Equation (3.6) can be used to calculate energy losses of a 20-cell battery with normal cell capacity distribution at different capacity variations. Fig. 3.3 shows the obtained graph. 10 sets of random normal distribution capacities were generated for each of capacity variation points from 0.5 % to 4 %. The line shows average energy losses while the dots mark the max and min losses

of performed calculations. If capacities of battery cells have normal distribution, then balancing losses will increase linearly with increase in cell capacity variation.

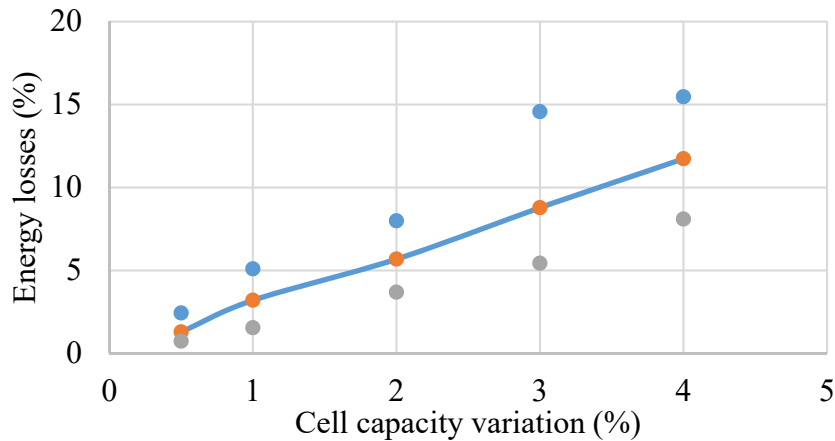


Fig. 3.3. Energy loss of a 20 cell battery with switched resistor balancing at different cell capacity variation levels.

Despite the overall criticism of inefficient operation, there are multiple scientific publications that utilize variations of the switched resistor balancing [26], [24], [27]. Traditionally, switched resistor balancing is regarded as an inefficient method, and many other methods are proposed as better alternatives [22], [21], [23], [28], [29]. However, multiple commercial products are available and are actively implemented in battery pack design.

A perspective type of selective charge/discharge is the multi converter based balancing method. These converters are regarded as full-bridge multilevel converters or modular multilevel converters. The basic principle is that each cell [30] or a group of cells [31] is equipped with a bidirectional converter (typically a full-bridge converter) and the outputs of the converters are series connected to build the series string of the battery. By controlling the individual converters each cell can be selectively charged, discharged or completely bypassed, if needed. One of the special advantages is that this system can be used as the main converter – the cascaded H-bridge multilevel inverter. The inverter can be used to supply motors [32], [33] or to be connected to the grid [30], [34], [31]. As each converter consists of semiconductor switches, there are additional losses – mostly conduction losses. As noted in [30] the use of underutilized MOSFETs leads to additional losses to the overall system. The other main challenge of this balancing method is related to control. First, it has to estimate the SoC of each cell, which is more complicated if compared to other methods because the charge/discharge current is different for each cell.

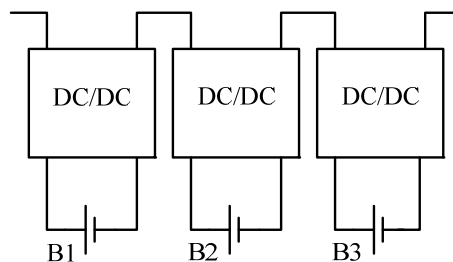


Fig. 3.4. Multi converter balancing topology.

A well-known capacitor based method is called switched capacitor balancing method (Fig. 3.5) [35], capacitor shuttle balancing method or charge shuttling [36], [37], [38]. The total capacitor count is $n - 1$, where n is a cell count. The circuit uses only bidirectional SPDT switches, and switch count is the same as the cell count. This method can transfer energy from one cell to the next (next-to-next balancing), thus a major disadvantage is the low equalization speed and poor efficiency if the mismatched cells are far apart in the stack. However, a significant advantage over the single capacitor version is the easy modularization feature [23]. The equalization time of this method can be improved by adding one extra capacitor and a set of switches, which allow to connect this capacitor to the first and last cells of the stack [39], thus making a full balancing loop. The switched capacitor method can be designed to be double-tiered. The additional capacitors permit energy transfer between cells that have one cell in between. The second tier decreases both voltage equalization time and energy losses.

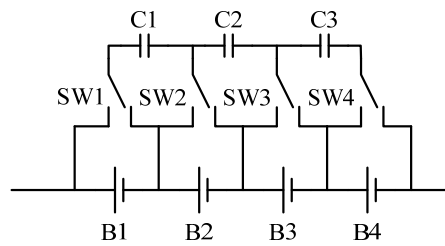


Fig. 3.5. Switched capacitor balancing topology.

A well-known inductor based balancing topology is buck-boost converter based topology [23], [40], [28], [41], [42]. The basic topology with two individual cell equalizers is shown in Fig. 3.6. It performs charge transfer from cell-to-cell between cells that are next-to-next connected. An individual cell equalizer is connected to a pair of cells, thus for n series connected cells there are $n - 1$ cell equalizers required. The buck-boost based topology has disadvantages of high current ripple and narrow duty cycle variation for balancing operation. However, this method requires only one inductor and no capacitor per individual cell balancer, which makes it cheaper, smaller, and easier to design and implement. It has been implemented as commercial product [43].

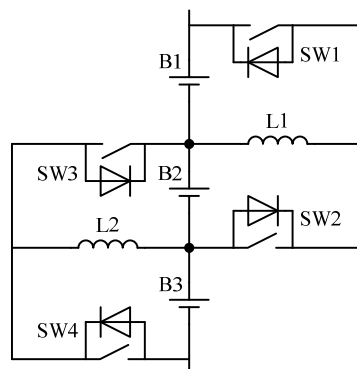


Fig. 3.6. Buck-boost (next-to-next) based balancing topology.

Shared transformer method is commonly referred to as multi-winding transformer method, as the main transformer has multiple secondary windings – one for each cell or one for a pair of cells [44], [45]. Fig. 3.7 shows a reference version of a multi-winding transformer balancing

topology that supplies primary side converter directly from the pack, while a winding and a diode is used to transfer energy to each cell. A number of converters can be used for primary side [45], [46], [45], [47], [48]. The DC/DC converter could be fed from the battery pack or from the DC-link of the charger. Significant emphasis is put on the design of transformer, as it is the most complex and limiting component of the topology. However, the complexity of the transformer usually is mentioned as the main drawback of multi-winding topologies [21], [49].

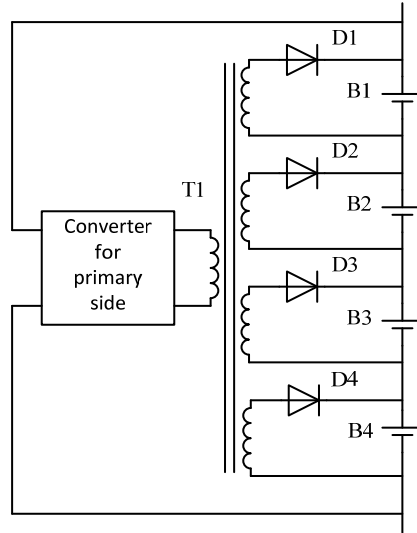


Fig. 3.7. Multi-winding transformer balancing reference topology.

One of the conclusions from this review is that dissipative balancing is inefficient and should be avoided [50], [51], [52]. This motivation assumes that balancing will be performed once the cells have high SoC mismatch. Up to 0.5 V voltage [51] and 42 % SoC [53] mismatch is used to validate the proposed balancing circuits. However, in practical battery packs cells are balanced during every charging procedure, which, in turn, minimizes the cell voltage mismatch at the end of next discharge [54]. The reasons for cell voltage balancing are that it is a lot easier to just measure each cell's voltage and fresh cells should not have higher capacity mismatch than 3 % (typical information from manufacturers datasheets [55]) which is relatively easy to balance. Test results in [54] show that for up to 500 cycles the charge/discharge efficiency of a balancer-less multi-cell battery is practically the same as if the battery would be equipped with a balancing circuit – this adds to the conclusion that switched resistor balancing is eligible even for modern battery packs.

Overall multi-layer or multi-stage balancing is rarely researched. Some proposals are presented in [56] and [57], where small DC/DC converters are used to balance cells within a battery module, while a more powerful DC/DC converter is used to transfer energy from the small converters to the whole battery pack. Similar work has been done in [58] and [59], where a balancing topology is used to perform balancing of individual cells and additionally perform balancing of cell modules. Here the proposed term is modularized balancing, as the battery is divided into modules where dedicated balancing circuits transfer energy between them. Such dual-balancing or mixed-balancing approach can effectively be used to gain on advantages of different balancing topologies.

4. INVESTIGATION OF INDIVIDUAL CELL TESTING METHODS

As the goal of this Thesis is to design and implement a battery pack with BMS for a small vehicle, the first experimental step is to obtain measurement data regarding individual cells. For the first test, the capacity (40 Ah nominal) of nine LFP *WB-LYP40AHA* cells was measured at different charging voltages [60], [61]. Cells were charged to three levels: 3.6, 3.7 and 3.8 V. The obtained capacity readings are shown in Fig. 4.1. The average capacity at 3.8 V is 40.93 Ah, at 3.7 V it is 40.12 Ah, and at 3.6 V it is 40.07 Ah. The difference between 3.8 V and 3.6 V charging is 2.08 %. Since the decreased operational voltage range improves the cycle life, it is beneficial to use smaller charging voltage.

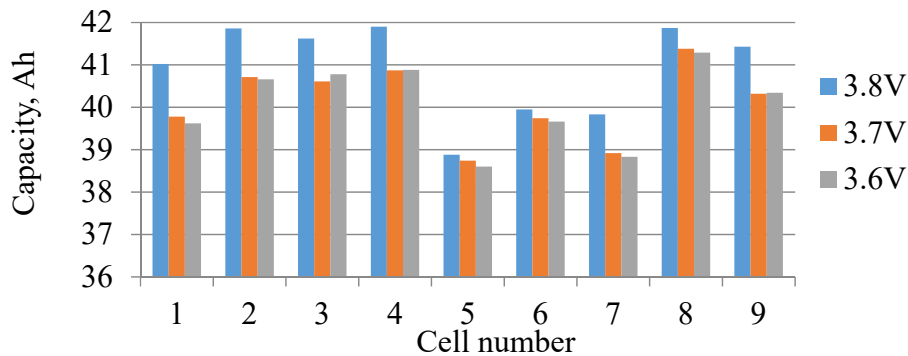


Fig. 4.1. Capacity of 9 LFP cells at different charging voltages.

For the next test, the same nine cells were tested for open circuit voltage (OCV). The obtained OCV graph is shown in Fig. 4.2. After charging and relaxation, for the first point (0 Ah) all cells were at $3.6 \text{ V} \pm 1 \text{ mV}$. All readings are well grouped, however, at 10 Ah discharge and after 25 Ah discharge, some voltage difference is noticeable. At 10 Ah max difference is 7.4 mV, at 25 Ah it is 4.9 mV, at 30 Ah it is 10.4 mV, at 35 Ah it is 16.3 mV, and at final 40 Ah it is 33.7 mV. The obtained graph indicates that if cell balancing is done during the end-phase of charging, then there is a relatively small change in charged capacity per mV of cell's voltage, hence there is no need for high resolution measurements of battery's cells volages.

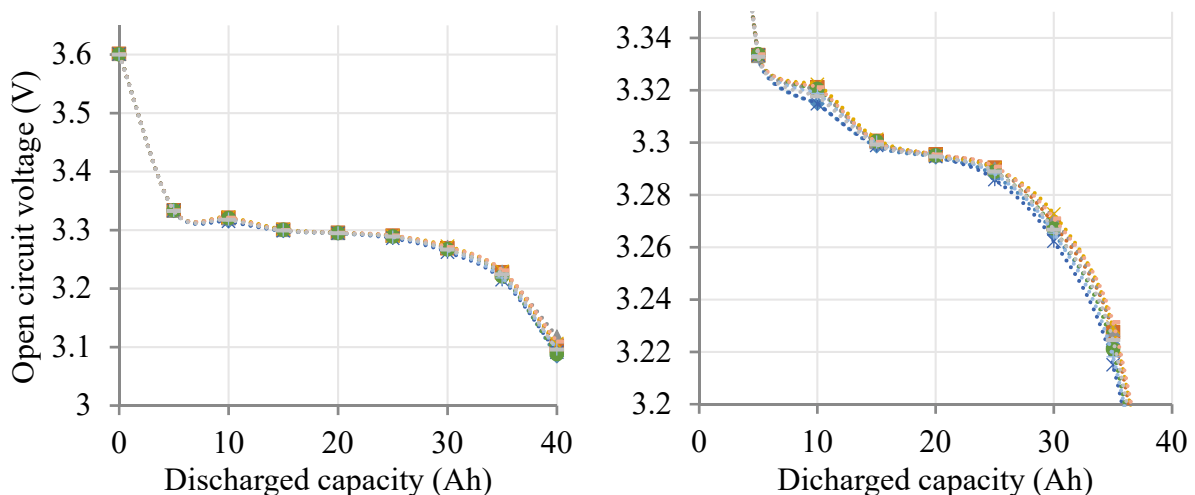


Fig. 4.2. OCV of 9 LFP cells: left – full span; right – zoom-in on central region.

Four 83 cell batches of 18650-size cells were purchased as part of a research project to develop a customizable power-assist wheelchair. The basic specification of these models is given in Table 4.1.

Table 4.1

Basic Specification of the Tested 18650-size Cells

Manufacturer	Model	Cap, Ah	Cycle life	Dch current, A	Chg current, A
Sony	US18650VTC6	3.13	500	20	3
LG Chem	INR18650MJ1	3.5	400	10	1.7
Samsung SDI	INR18650-35E	3.35	500	8	1.7
Panasonic	NCR18650GA	3.3	300	10	1.475

The initial capacity of all 332 cells was measured to obtain information about the capacity dispersion within the batches. Statistical methods were implemented to analyze the obtained measurements. For *INR18650MJ1* the range of the capacity value can differ a maximum up to 5 %, which is slightly higher than the 3 % range given by the manufacturer. For *US18650VTC6* the range was only 2.03 % and for *INR18650-35E* the range of the capacity values can differ 2.31 %, while for *NCR18650GA* the values differed in 2.74 % range. This data shows that within all models, except *INR18650MJ1*, choosing any random cells for one battery the difference between the cells will never be greater than 3 percent. It can be assumed that in these cases the application of resistive balancing during charging process would not generate high energy losses. A descriptive box and whisker plot is shown in Fig. 4.3.

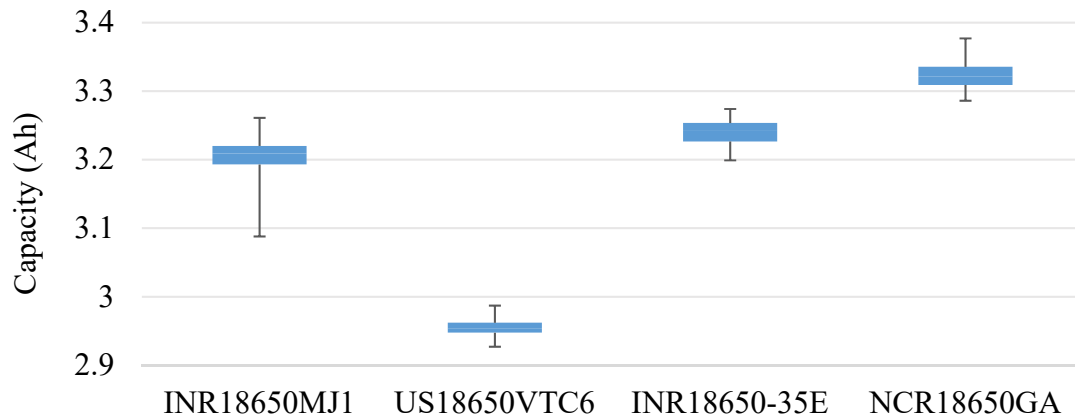


Fig. 4.3. Box-whiskers plot for comparison of different capacities of selected cell models.

Additional calculations were made regarding the option what would be the best optimal battery cell pack of 28 cells when selecting the cells of each battery type knowing the measured data. For *INR18650MJ1* the optimal chosen working capacity would be 3.210 \pm 0.006 Ah (0.187 % range). For *US18650VTC6* the optimal chosen working capacity would be 2.955 \pm 0.004 Ah (0.135 % range). For *INR18650-35E* the optimal chosen working capacity would be 3.243 \pm 0.007 Ah (0.231 % range). And for *NCR18650GA* the optimal chosen working capacity would be 3.323 \pm 0.006 Ah (0.181 % range). By comparing the randomly chosen battery back with a specifically chosen one, the difference in the range and the precision of the battery pack capacity is more than ten times larger.

Another estimation is the likelihood of obtaining a 28-cell battery pack with certain cell capacity range by random cell selection. For *US18650VTC6*, *INR18650-35E* and *NCR18650GA*, the capacity mismatch range is below 3 %, while the probability to obtain a 3 % range from *INR18650MJI* cells is just 1.9 %. The probability of a 2 % cell capacity range mismatch is 66.2 % for *US18650VTC6*, impossible for *INR18650MJI*, 18.5 % for *INR18650-35E* and 7.6 % for *NCR18650GA*. It was calculated that the probability to obtain a battery pack with a cell capacity range below 1 % is less than 0.1 %, or impossible for all cell models.

Capacity measurement is a time-consuming process, as it requires charging (up to 2.5 hours) and discharging (more than 1 hour) of each cell. Another battery parameter is measurable faster – the impedance. It was measured at four frequencies (1, 10, 100, 1000 Hz) and three SoC levels (100 %, ~70 %, ~30 %). Statistical calculations were made for all data sets. The main factors that were calculated for these data sets were mean, standard error, median, standard deviation, sample variance, range, confidence level, and fluctuation against the mean. Also, for the data sets, normal distribution plots (Fig. 4.4) were distributed and compared. The impedance results were compared to the results of capacity to see if there is any correlation between the impedance and capacity variation.

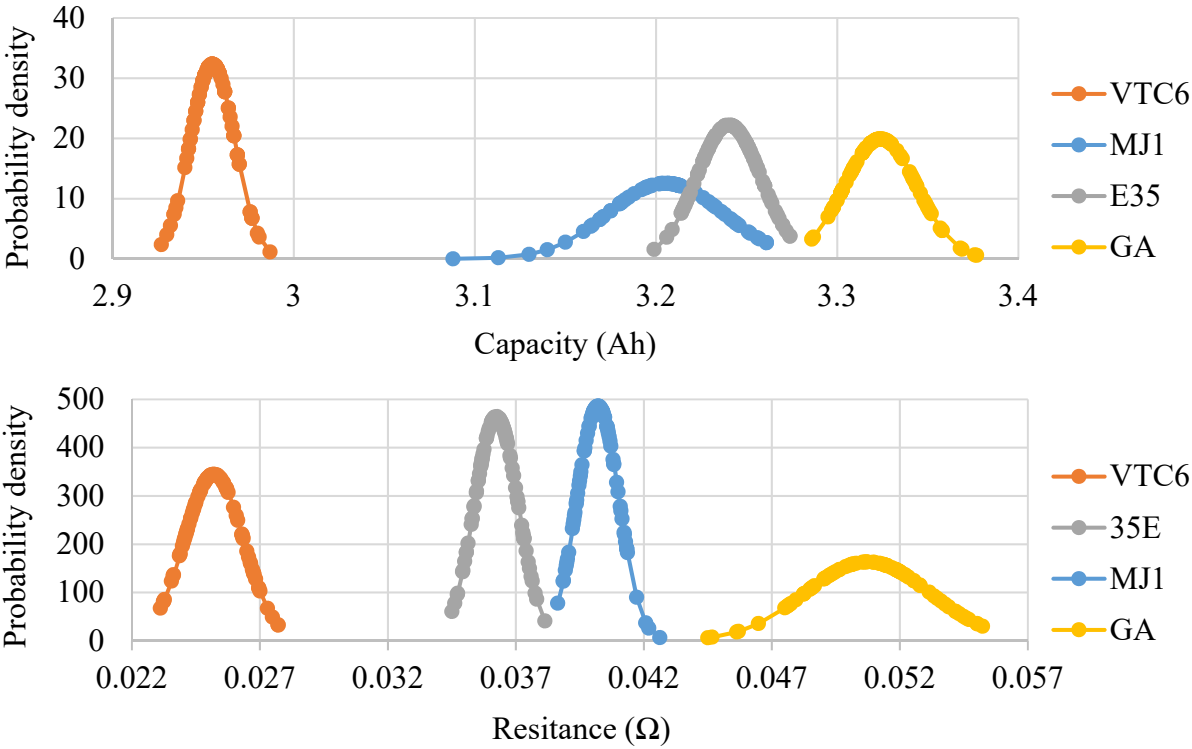


Fig. 4.4. Normal distribution plot for capacity (top) and for impedance (bottom).

The direct correlation between the capacity and impedance was calculated in each model of cells. Two cell models show that there is a 20 % or more correlation. *INR18650MJI* shows an 11 % correlation and *NCR18650GA* showed only 1 % correlation. The calculated straight correlation between the capacity and impedance proved to be moderate in the cases of *US18650VTC6* and *INR18650-35E*, while in the case of *INR18650MJI* and *NCR18650GA* the correlation was weak. It can be concluded that the impedance measurements are not applicable to direct cell sorting according to capacity.

5. THE DEVELOPMENT OF A BATTERY CONFIGURATION FOR A PMV

Part of the Doctoral Thesis was devoted to design a 320 W battery pack for a PMV: a powered wheelchair. First, basic product information was obtained for 34 commercial wheelchairs. Then, the power consumption and battery specification was analyzed. It was estimated that 24 V 480 Wh battery would be sufficient to achieve the set goals. 115 shop articles were analyzed and compared to select Li-ion cells suitable for the battery pack. It was decided to use 18650-size cells with at least 3 Ah capacity to fit weight and size constraints while providing some design flexibility. The final selected cell models are given in Table 4.1.

A set of cells can be arranged in finite configurations. As shown in (5.1), where the left side represents the series connection and the right side parallel configuration, conduction losses are not affected by configuration. Hence, other system power losses should be considered when selecting optimal battery pack voltage.

$$\frac{P_{batt}^2 \cdot R_{cell} \cdot n_{cell}}{U_{cell}^2 \cdot n_{cell}^2} = \frac{P_{batt}^2 \cdot R_{cell}}{U_{cell}^2 \cdot n_{cell}} \quad (5.1)$$

An analysis of the motor design was made to find the optimal voltage. Motor linear load and slot fill factor was analysed in respect to nominal voltage – it was confirmed that a motor can be designed if the nominal voltage is in the range of 18 V to 36 V. A slot fill factor limits motor design as shown in Fig. 5.1

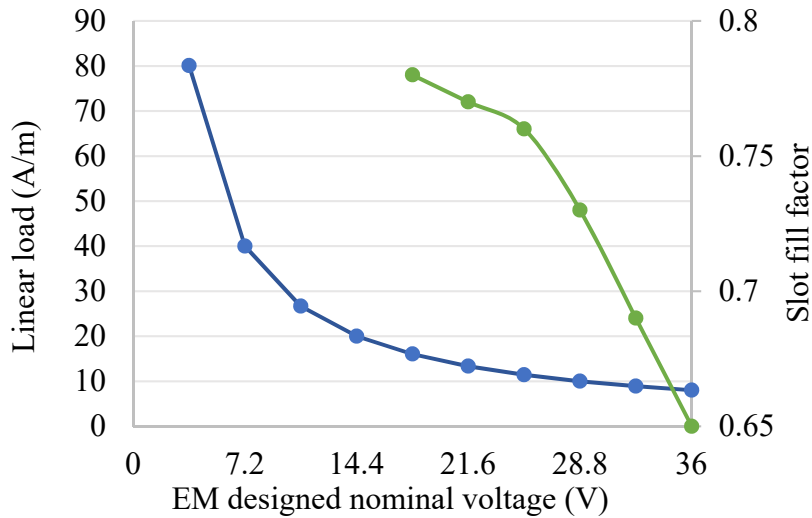


Fig. 5.1. Calculated linear load (green) and armature slot fill factor (blue).

A typical motor driver is a voltage source inverter, which is directly fed from the battery pack. The nominal voltage of the battery pack has direct impact on the electrical parameters of the inverter, hence MOSFET losses (Fig. 5.2) were analysed at each possible battery voltage level (a total of 10 levels) to find optimal nominal voltage. It can be concluded that above 7.2 V nominal voltage, the configuration of the battery pack has no impact on the losses of the drive's semiconductor switches. Similar conclusion was drawn when analysing the losses of multi-converter isolated SEPIC converter-based battery charger. MOSFET cost analysis revealed that the lowest cost is if voltage is between 14.4 and 32.4 V.

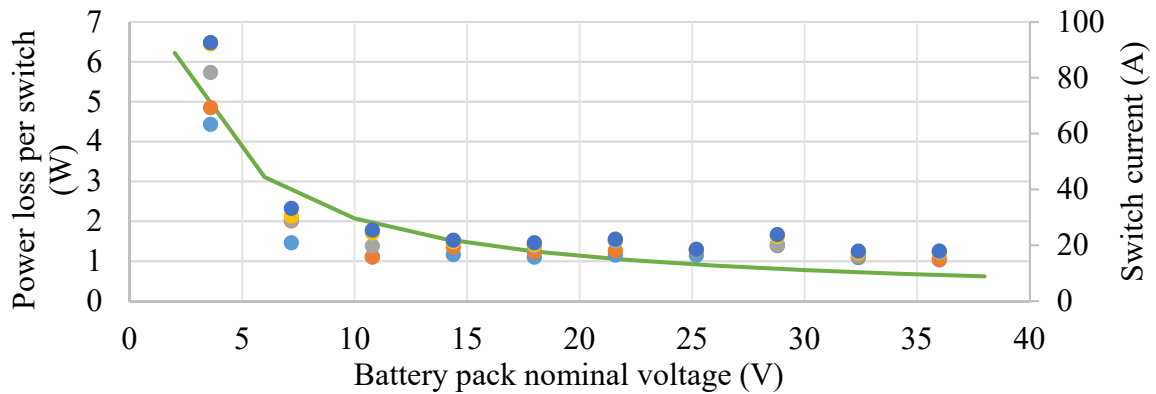


Fig. 5.2. Calculated power loss (dots) and current (line) per motor inverter switch at different nominal battery voltages.

The battery pack would minimally consist of 25 cells, however, 28 cells allow for more flexibility. Table 5.1 summarizes all configurations if a minimum of 28 cells at 3.6 V each is used. A full charge voltage of 9S4P and 10S3P configurations exceeds 36 V – for safety, these configurations should be avoided. This leaves configurations 4S7P and 7S4P. 4S7P should not be used because a 14.4 V nominal voltage is not suitable for the motor design, which requires the voltage to be higher than 18 V. The 7S4P configuration is the best choice, as the nominal voltage is high (current is low), while the losses and price of semiconductors are relatively low. 5S5P – a 25 cell configuration – would be marginally sufficient for motor requirements, and it would lack the possibility to switch to other (smaller capacity) cells and would not be backwards compatible with 12V-based lead-acid battery systems – this is an additional feature of the 7S4P configuration. To conclude, it was decided that the 7S4P configuration is best suited, as it provides good performance and flexibility at the cost of 3 extra cells.

Table 5.1

Parameters of Battery Pack at Different Cell Configurations

Nominal voltage (V)	Full voltage (V)	Current (A)	Battery configuration	Required cells	Drive losses	Charger losses	MOSFET price
3.6	4.2	88.9	1S28P	28	High	High	High
7.2	8.4	44.4	2S14P	28	Average	Average	Average
10.8	12.6	29.6	3S10P	30	Low	Average	Average
14.4	16.8	22.2	4S7P	28	Low	Low	Low
18	21	17.8	5S6P	30	Low	Low	Low
21.6	25.2	14.8	6S5P	30	Low	Average	Average
25.2	29.4	12.7	7S4P	28	Low	Low	Low
28.8	33.6	11.1	8S4P	32	Low	Average	Average
32.4	37.8	9.9	9S4P	36	Low	Low	Average
36	42	8.9	10S3P	30	Low	Average	Average

6. CELL BALANCING SYSTEM DEVELOPMENT AND VERIFICATION

The key goal of this Thesis was to develop a balancing system for another electric vehicle: electric kart, which uses two battery packs each consisting of twenty 40 Ah LFP cells. Initially, a switched resistor balancing method was implemented, which was then upgraded with a transformer-based charge transfer to develop a novel multi-stage balancing method. The balancing system was designed using modular concept with single master controller.

There were three iterations (Fig. 6.3) of cell module development, which made improvements on board design and control software. The cell module board was designed to fit on top of the selected LFP cell. Each iteration used a slightly different approach of shunting resistor execution: a set of series connected resistors, a suspended resistor, and, finally, a single resistor with board cutouts for improved thermal isolation. Hardware was designed to support a daisy chain communication. The initial cell module used an optocoupler to isolate the communication line, while the final module version used a more efficient resistor divider. The power consumption of cell module was gradually reduced from 2.9 mA to 0.9 mA.

Two separate parts can be distinguished from the program operation point of view. The first part could be described as the main operation phase, while the other part is used to perform data transfer using UART communication. In the first part, during the initialization, ADC is set to perform cell voltage measurements and then save the filtered average value in TX buffer and use it for switched resistor activation.

Special care was taken to calibrate the ADC of each module. Initial accuracy of 20 module measurements are shown in Fig. 6.1. The dispersion spans across 30 discrete values – the cell voltage measurement can have 12 % error.

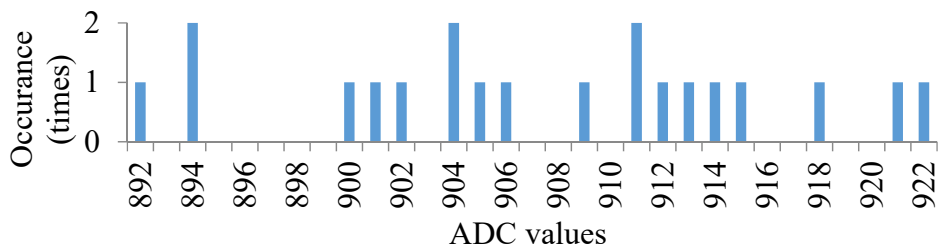


Fig. 6.1. ADC conversion values from 20 cell balancer modules.

By utilizing slope equalization using a dedicated calibration setup it was possible to improve voltage measurement consistency, as shown in Fig. 6.2, to produce 0.8 % error. The calibration procedure was extended to include temperature measurement calibration. The module software was updated to include calibration routine during initial start-up.

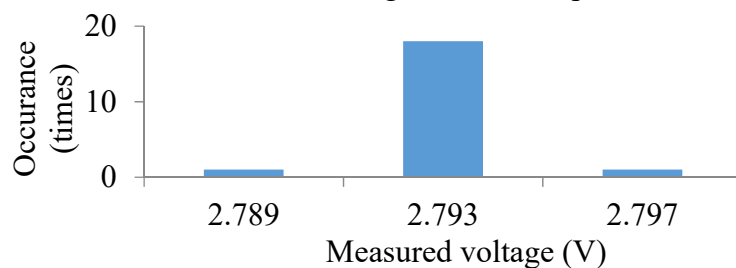


Fig. 6.2. Display readout dispersion with ADC slope compensation.

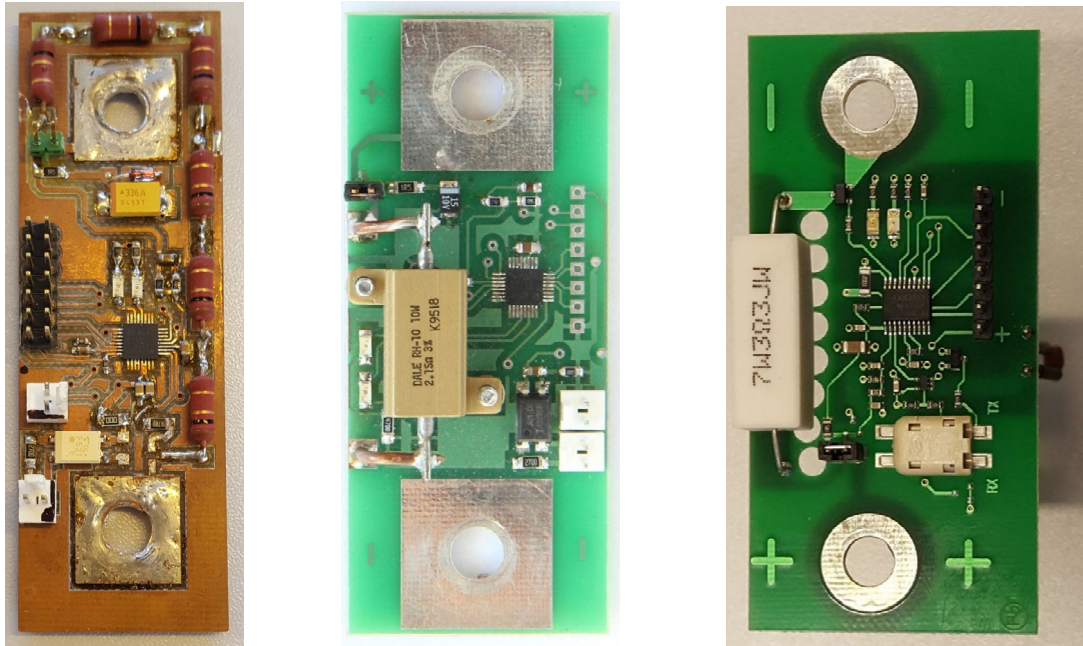


Fig. 6.3. Assembled cell modules: left – the first; centre – the second; right – final.

Two editions of master module were designed to test the balancing performance. The final edition (Fig. 6.4) was equipped with an LCD to show voltage values and a micro SD card to store the received cell data in raw format, which was later processed using *HxD editor* and *Matlab*. A real time clock was used to initiate data exchange at exact intervals so that it would be possible to produce cell voltage graphs.

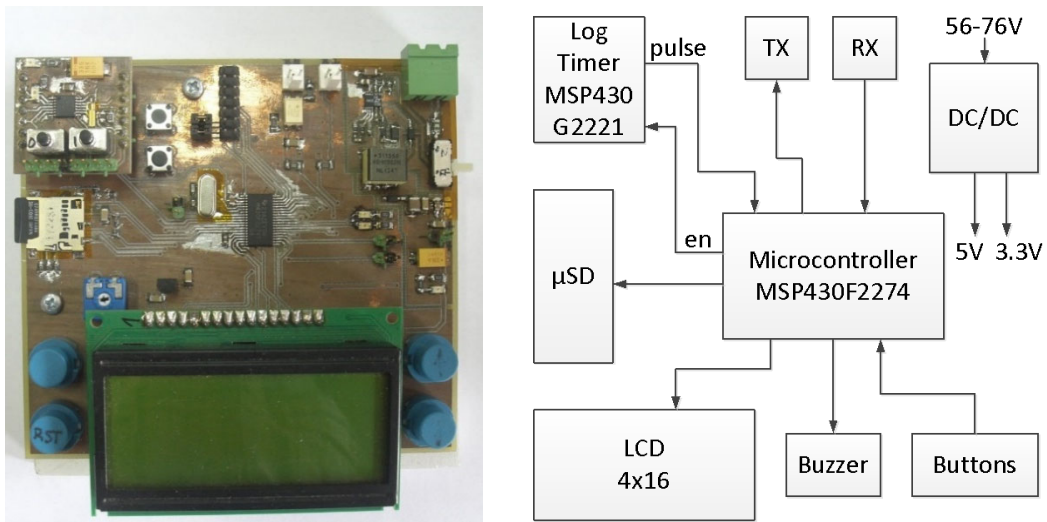


Fig. 6.4. BMS master module.

The developed balancing system was tested using a 20 cell 40 Ah battery. For the first BMS test, the pack was discharged at a 20 A rate (0.5C). The discharging was stopped once the BMS registered a cell reaching 2.8 V limit. The discharge voltage plot is shown in Fig. 6.5. The difference in cells voltages becomes apparent quickly, however, only during the last quarter the voltage of cell No.19 decreases rapidly, indicating a relatively lower capacity. Voltage of all cells increases after the discharge is stopped.

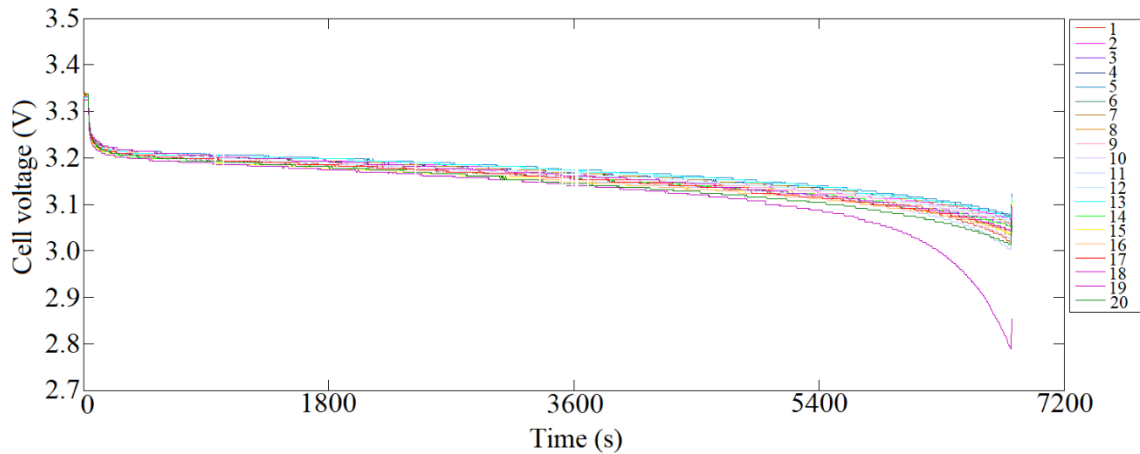


Fig. 6.5. Voltages of cells from BMS memory during discharging.

Next, the empty battery pack was charged with 11 A. Fig. 6.6 shows the obtained graph of voltages. It can be seen that during the final phase of the charging one of the cells reaches 3.9 V, while voltages of other cells fluctuate around 3.8 V. At this point the 11 A charging current is higher than the balancing current, and as the charging continues, the voltages of some (fuller) cells can rise above set 3.8 V limit. After the 3.9 V peak, the charging current was manually decreased to 1.5 A, resulting in voltage decrease of all cells. However, soon afterwards the voltages of cells again reach the 3.8 V limit, as they have become fully charged.

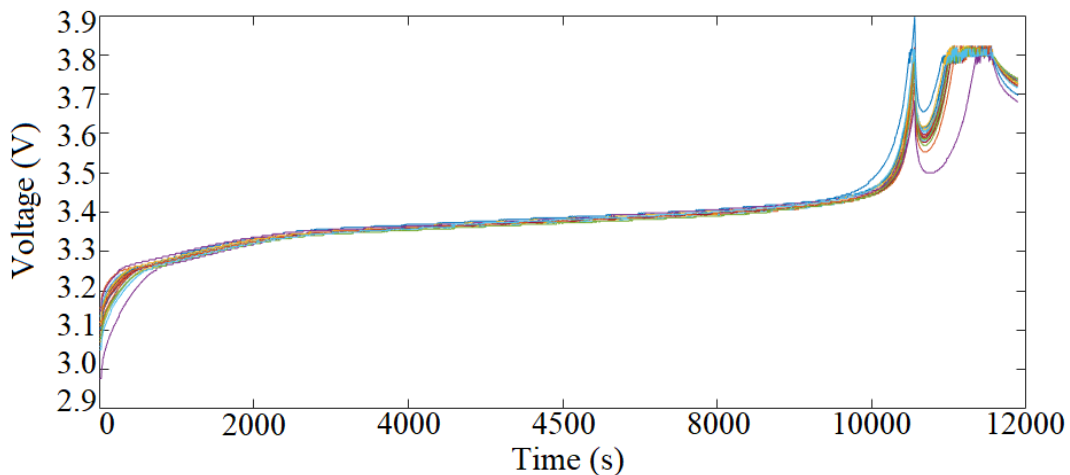


Fig. 6.6. Voltages of cells from BMS memory during charging.

It was measured that the given LFP battery has 93 % efficiency over 10 charge/discharge cycles. Approximately 1.2 % of charging energy was lost during the switched resistor balancing. It can be concluded that under given circumstances the developed cell balancing system has small losses, while being simple and easy to implement in modular approach.

7. DEVELOPMENT OF ADVANCED CELL BALANCING

Drawbacks of switched resistor balancing could be minimized if cells of the battery are grouped in smaller groups and charged separately. Grouped cells of a battery pack can be charged with a single multi-secondary winding transformer – this approach provides inherent charging current distribution according to cell group voltage. The result is a two-layer balancing scheme.

To verify the operation of the multi-secondary winding transformer, it was decided to build and test a three-cell charger circuit with max charging current 10 A, using supercapacitors instead of battery cells. A half-bridge topology was selected for the primary side, while each winding of the secondary side was equipped with a rectifier and an LC filter as shown in Fig. 7.1. If duty cycle is kept constant, then the cell current is inversely proportional to its voltage, and thus its state of charge. Since all cells are in the same system, the cell with the lowest voltage will have the largest current. Because of this effect, this balancing technique is capable to balance cells without additional closed feedback loops [62].

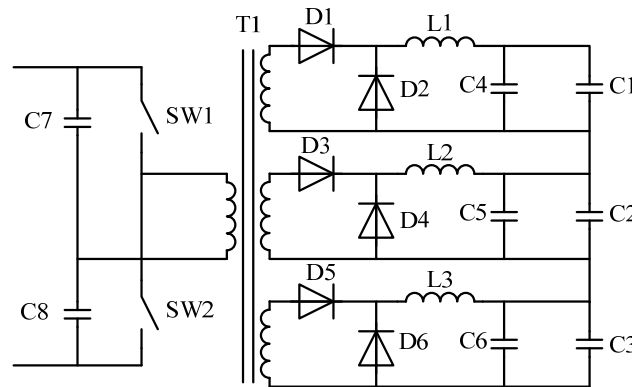


Fig. 7.1. Multi-secondary winding battery charger circuit for three cells.

Three tests were performed: with equally discharged caps, with one cap having double capacitance, and with different initial voltages. During the first test, caps were charged to 30 mV difference. During the second test, the initial 180 mV was reduced to 58 mV. The third test successfully balanced the caps with initial voltages: 1.5 V, 1.0 V, and 0.5 V (Fig. 7.2). The self-balancing feature is depicted in the graph, as all cells reach the same end voltage at the same time. It can be concluded that the given multi-secondary winding transformer charger-balancer is a suitable choice for the top layer of the proposed mixed multi-layer topology.

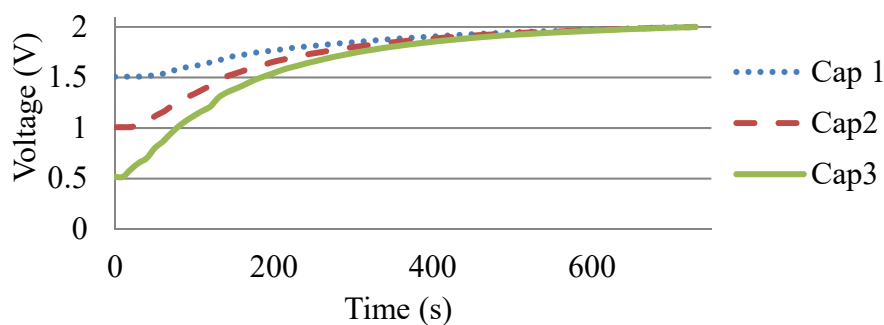


Fig. 7.2. Charging of capacitor cells with different initial voltages.

Before proceeding with testing of the two-layer mixed balancing system, a benchmark test of switched resistor balancing was performed. *N4L* precision power analyser *PPA5530* was used to measure the energy drawn from the battery. The total energy was 2.45 kWh, and additional measurement indicated that the battery was discharged for 38.7 Ah. Then, a half-bridge converter was used to fully charge the battery at 10 A. The total amount of energy spent during the charging was 3.01 kWh. The energy used for the driver and control circuitry was not taken into account. For this system the energy efficiency was 81.4 %.

A similar efficiency test was carried out with a mixed two-layer balancing topology. Four secondary windings were connected to subpacks: each 5 cells of the pack constituted a subpack. The schematic of the setup is shown in Fig. 7.3. Both charging and discharging energy was measured to estimate efficiency.

The experimentally obtained results are as follows: the energy required to fully charge the battery pack was measured to be 3.09 kWh, and the process took 4 hours and 38 minutes; during the discharge, the obtained energy amount was 2.43 kWh and the process took 3 hours and 50 minutes. During the discharge an additional battery pack capacity measurement was done, and the battery pack measured to have a 38.34 Ah capacity. From both measurements it can be calculated that the energy efficiency of the battery pack with charger and integrated mixed two-layer balancing is 78.6 %.

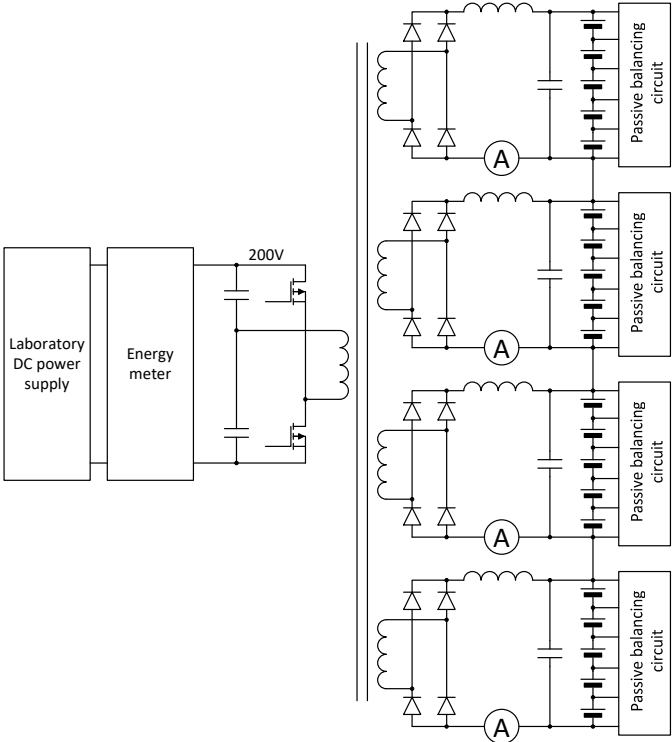


Fig. 7.3. The schematic of the charger with an integrated mixed balancing function.

It can be concluded that the developed mixed balancing method is capable to successfully utilize a multi secondary transformer balancer for higher layer balancing, while the switched shunting resistor balancing takes care of the lower layer balancing. However, the test revealed that the overall system energy efficiency is 78.6 %, while the previously tested efficiency of a switched shunting resistor balancing was 81.4 %. The introduction of additional windings and

rectifiers have lowered the converter efficiency, thus decreasing the energy efficiency measurement. From another perspective, the energy efficiency should increase due to split switched resistor balancing. The cells of the battery pack are split into 4 subpacks – the switched balancing losses should decrease, as the number of cells to balance per subpack is smaller. If randomly generated cell values are used for battery pack which is split into 4 subpacks, then the switched balancing losses decrease, as shown in Fig. 7.4. with line $4 \times 5S$ (series connection of 4 subpacks each consisting of 5 series connected cells). It can be concluded that the packs with higher cell capacity variation will benefit more from mixed balancing topology.

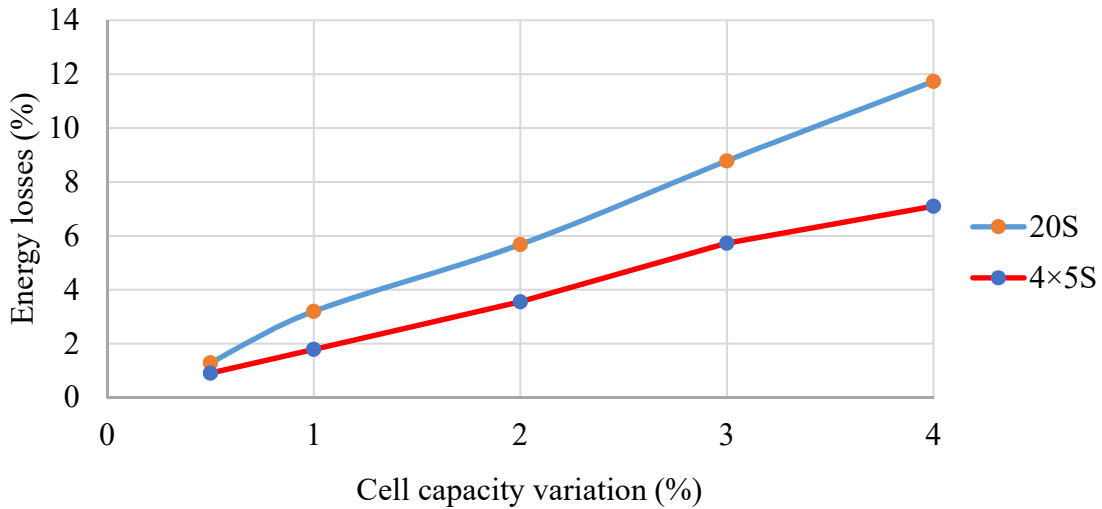


Fig. 7.4. Battery energy losses with full switched resistor balancing (20S) and split switched resistor balancing ($4 \times 5S$).

If the achieved split switched resistor balancing loss improvement is larger than the additional losses of multi secondary winding transformer (7.1), then the mixed two-layer balancing will provide energy improvement over the conventional switched resistor balancing:

$$E_{MST} < E_{SR_full} - E_{SR_split}, \quad (7.1)$$

where

E_{MST} – energy loss of multi secondary winding topology, Wh;

E_{SR_full} – energy loss of conventional switched resistor balancing, Wh;

E_{SR_split} – energy loss of split switched resistor balancing, Wh.

As the battery is split into more subpacks, energy loss E_{SR_split} is decreased and the advantage of multi secondary transformer introduction increases. The E_{SR_split} value will decrease to 0 if an individual winding is used for each cell – the switched resistor balancing layer loses its purpose. However, it can be troublesome to achieve a sufficiently low E_{MST} value, as the multi-secondary transformer topology related losses are generated throughout all charging procedure as opposed to the switched resistor topology, which generates losses only after the first cell has reached its full voltage. The losses of multi secondary transformer topology should be optimized to achieve minimal losses at max transformer utilization to permit successful application of mixed two-layer balancing.

CONCLUSIONS

To achieve the set goals, the work was started with the analysis of various electric vehicle battery systems. From the available material, it can be concluded that the voltage of the traction battery corresponds to the one of the drive system. On few occasions, a rudimentary BMS analysis was possible, as the image of BMS board was available – it yielded that the switched resistor balancing method was used in all of the reviewed cases.

Research literature analysis on BMS and balancing methods was conducted. A novel balancing method categorization was designed with three main sections: dissipative methods, selective charge/discharge methods, and charge transfer methods. The first finding regarding balancing methods is that dissipative (e.g., switched resistor) methods are regarded as inefficient, and hence they should be avoided, although no proof with real world battery parameters were observed. The second finding is that no mixed multi-layer balancing methods were observed during the literature review.

An experimental Li-ion battery performance analysis was carried out. The capacity analysis indicated that it is possible to achieve high initial cell capacity match (less than 0.2 % mismatch) if the cells are sorted according to actual capacity. The capacity measurement is inherently a time-consuming process, although in some cases it could partially be replaced by much faster impedance measurement, which correlates to capacity.

Switched resistor cell balancing modules for 40 Ah LFP cells have been designed. A measurement calibration procedure has been developed and integrated in embedded system. The performance of the designed BMS has been verified with a 20-cell LFP battery pack. After a full discharge, a charging cycle took 240 minutes of which the balancing lasted less than 16 minutes, which indicated a short balancing time. The cell voltage measurement analysis showed that a single cell of the pack was the major reason for given balancing activity. The balancing requirement could have been decreased if the cells were sorted prior to the pack assembly.

The performance of a multi-secondary winding transformer balancing method has been experimentally validated using a 3 EDLC pack. Further, a half bridge transformer topology with four secondary windings was used to test the performance of mixed two-layer balancing topology. The 20-cell LFP battery was divided into four groups with switched resistor balancing modules for the lower layer. The energy efficiency was 78.6 %, while the previously tested efficiency of switched shunting resistor balancing was 81.4 %. A conclusion can be drawn: the combination of the given two balancing methods does not provide higher energy efficiency at given cell capacity parameters. The defined hypothesis is true if the loss improvement of split switched resistor pack is larger than the additionally introduced multi secondary winding topology losses.

Future work includes continuation of work in the field of battery applications and their management systems. The developed BMS and 40 Ah LFP battery pack is to be used for educational electric kart project with multiple independent drives. It is planned to design battery packs for other PMV development projects. Another future research direction is related to the development of cell parameter measurement systems – to measure the cell parameter change as they are being aged. The obtained statistical knowledge is to be used to develop model-based SoC and SoH estimators for future BMS.

REFERENCES

- [1] CSDD, “Statistics of registered vehicle.” [Online]. Available: <https://www.csdd.lv/en/vehicles/statistics-of-registered-vehicle>.
- [2] “A European Green Deal | European Commission.” [Online]. Available: https://ec.europa.eu/info/strategy/priorities-2019-2024/european-green-deal_en. [Accessed: 29-Oct-2021].
- [3] N. Smith, “Beyond Energy: The Main Offenders [Climate Change Energy],” *Eng. Technol.*, vol. 15, no. 10, pp. 30–33, Nov. 2020.
- [4] “Electric Race Car Design & Engineering – Drive eO.” [Online]. Available: <https://driveeo.com/>. [Accessed: 01-Nov-2021].
- [5] “Electric Racing Karts – Blue Shock Race Electric karts.” [Online]. Available: <https://blueshockrace.com/electric-racing-karts/>. [Accessed: 01-Nov-2021].
- [6] “e-up! for everyone – new generation of the electric e-up! with a long range to be launched at a low price | Volkswagen Newsroom.” [Online]. Available: <https://www.volkswagen-newsroom.com/en/press-releases/e-up-for-everyone-new-generation-of-the-electric-e-up-with-a-long-range-to-be-launched-at-a-low-price-5318>. [Accessed: 27-Jun-2020].
- [7] “2018 Nissan Leaf battery technology, a deep dive.” [Online]. Available: https://www.greencarreports.com/news/1117928_2018-nissan-leaf-battery-technology-a-deep-dive. [Accessed: 27-Jun-2020].
- [8] “BMS and contactor box – AEVA Forums.” [Online]. Available: <https://forums.aeva.asn.au/viewtopic.php?t=4278>. [Accessed: 27-Jun-2020].
- [9] “Bmw i3 bms | DIY Electric Car Forums.” [Online]. Available: <https://www.diyelectriccar.com/threads/bmw-i3-bms.198547/>. [Accessed: 01-Jul-2020].
- [10] “BMW i3 electric car battery balancing circuit (BMS) – Imgur.” [Online]. Available: <https://imgur.com/gallery/wdk7o/comment/1046244385>. [Accessed: 01-Jul-2020].
- [11] “Pics/Info: Inside the battery pack | Page 14 | Tesla Motors Club.” [Online]. Available: <https://teslamotorsclub.com/tmc/threads/pics-info-inside-the-battery-pack.34934/page-14#post-755546>. [Accessed: 27-Jun-2020].
- [12] “Tesla BMS Module – Front.jpg (6798×3415).” [Online]. Available: <http://files.wizkid057.com/teslapack/update2/Tesla BMS Module - Front.jpg>. [Accessed: 27-Jun-2020].
- [13] I. Tsiropoulos, D. Tarvydas, and N. Lebedeva, “Li-ion batteries for mobility and stationary storage applications,” 2018.
- [14] “Batteries for EBikes – EbikeMarketplace.” [Online]. Available: <https://ebikemarketplace.com/collections/lithium-batteries>. [Accessed: 18-Aug-2020].
- [15] “The Battery Doctor – YouTube.” [Online]. Available: <https://www.youtube.com/channel/UCxgrR15ORCLx7JI2MKqnmWw/videos>. [Accessed: 21-Aug-2020].
- [16] “Lithium-ion Battery Market Size and Share | Industry Analysis by 2027.” [Online]. Available: <https://www.alliedmarketresearch.com/lithium-ion-battery-market>. [Accessed: 19-Nov-2020].
- [17] “A Behind the Scenes Take on Lithium-ion Battery Prices | BloombergNEF.” [Online].

- Available: <https://about.bnef.com/blog/behind-scenes-take-lithium-ion-battery-prices/>. [Accessed: 04-Dec-2020].
- [18] “Lithium Ion Batteries Technical Handbook Japanese / International English,” vol. June. Panasonic, 2007.
 - [19] W. Xie *et al.*, “Challenges and opportunities toward fast-charging of lithium-ion batteries,” *J. Energy Storage*, vol. 32, no. August, p. 101837, Dec. 2020.
 - [20] S. Gantenbein, M. Schönleber, M. Weiss, and E. Ivers-Tiffée, “Capacity Fade in Lithium-Ion Batteries and Cyclic Aging over Various State-of-Charge Ranges,” *Sustainability*, vol. 11, no. 23, p. 6697, Nov. 2019.
 - [21] S. Moore and P. Schneider, “A Review of Cell Equalization Methods for Lithium Ion and Lithium Polymer Battery Systems,” in *SAE World Congress*, 2001, p. Doc. 2001-01-0959.
 - [22] M. Daowd, N. Omar, P. Van Den Bossche, and J. Van Mierlo, “Passive and active battery balancing comparison based on MATLAB simulation,” in *2011 IEEE Vehicle Power and Propulsion Conference*, 2011, vol. 6, no. 7, pp. 1–7.
 - [23] J. Gallardo-Lozano, E. Romero-Cadaval, M. I. Milanés-Montero, and M. A. Guerrero-Martinez, “Battery equalization active methods,” *J. Power Sources*, vol. 246, pp. 934–949, 2014.
 - [24] J. Gallardo-Lozano, E. Romero-Cadaval, M. I. Milanés-Montero, and M. a. Guerrero-Martinez, “Battery Equalization Control Based on the Shunt Transistor Method,” *Electr. Control Commun. Eng.*, vol. 7, no. 1, 2014.
 - [25] W. C. Lee, D. Drury, and P. Mellor, “Comparison of passive cell balancing and active cell balancing for automotive batteries,” in *2011 IEEE Vehicle Power and Propulsion Conference, VPPC 2011*, 2011.
 - [26] J. Gallardo-Lozano, A. Lateef, E. Romero-Cadaval, and M. I. Milanés-Montero, “Active Battery Balancing for Battery Packs,” *Electr. Control Commun. Eng.*, vol. 2, no. 1, pp. 40–46, 2013.
 - [27] J. Gallardo-lozano and E. Romero-cadaval, “A Battery Cell Balancing Method with Linear Mode Bypass Current Control,” in *2014 14th Biennial Baltic Electronic Conference (BEC)*, 2014, pp. 245–248.
 - [28] J. Cao, N. Schofield, and A. Emadi, “Battery balancing methods: A comprehensive review,” in *2008 IEEE Vehicle Power and Propulsion Conference, VPPC 2008*, 2008, pp. 3–8.
 - [29] J. D. Welsh, “A Comparison of Active and Passive Cell Balancing Techniques for Series / Parallel Battery Packs,” Ohio State University, 2009.
 - [30] E. Chatzinikolaou and D. J. Rogers, “Cell SoC Balancing Using a Cascaded Full-Bridge Multilevel Converter in Battery Energy Storage Systems,” *IEEE Trans. Ind. Electron.*, vol. 63, no. 9, pp. 5394–5402, Sep. 2016.
 - [31] C. M. Young, N. Y. Chu, L. R. Chen, Y. C. Hsiao, and C. Z. Li, “A Single-phase multilevel inverter with battery balancing,” *IEEE Trans. Ind. Electron.*, vol. 60, no. 5, pp. 1972–1978, 2013.
 - [32] S. D’Arco, L. Piegari, and P. Tricoli, “A modular converter with embedded battery cell balancing for electric vehicles,” in *Electrical Systems for Aircraft, Railway and Ship Propulsion, ESARS*, 2012.

- [33] F. Altaf, L. Johannesson, and B. Egardt, "Performance evaluation of Multilevel Converter based cell balancer with reciprocating air flow," in *2012 IEEE Vehicle Power and Propulsion Conference, VPPC 2012*, 2012, pp. 706–713.
- [34] A. Gholizad and M. Farsadi, "A Novel State-of-Charge Balancing Method Using Improved Staircase Modulation of Multilevel Inverters," *IEEE Trans. Ind. Electron.*, vol. 63, no. 10, pp. 6107–6114, Oct. 2016.
- [35] Z. Nie and C. Mi, "Fast battery equalization with isolated bidirectional DC-DC converter for PHEV applications," in *5th IEEE Vehicle Power and Propulsion Conference, VPPC '09*, 2009, pp. 78–81.
- [36] D. B. W. Abeywardana, M. a M. Manaz, M. G. C. P. Mediwaththe, and K. M. Liyanage, "Improved shared transformer cell balancing of Li-ion batteries," in *2012 IEEE 7th International Conference on Industrial and Information Systems, ICIIS 2012*, 2012.
- [37] Y. Barsukov, "Battery cell balancing: what to balance and how," *Texas Instruments*, 2005. [Online]. Available: [http://focus.ti.com/download/trng/docs/seminar/Topic 2 – Battery Cell Balancing – What to Balance and How.pdf](http://focus.ti.com/download/trng/docs/seminar/Topic_2_-_Battery_Cell_Balancing_-_What_to_Balance_and_How.pdf). [Accessed: 01-Jan-2015].
- [38] C. Pascual and P. T. Krein, "Switched capacitor system for automatic series battery equalization," in *Proceedings of APEC 97 – Applied Power Electronics Conference*, 1997, vol. 2, no. c, pp. 848–854.
- [39] M. Y. Kim, C. H. Kim, J. H. Kim, D. Y. Kim, and G. W. Moon, "Switched capacitor with chain structure for cell-balancing of lithium-ion batteries," in *IECON Proceedings (Industrial Electronics Conference)*, 2012, pp. 2994–2999.
- [40] T. H. Phung, J.-C. Crebier, A. Chureau, A. Collet, and V. Nguyen, "Optimized structure for next-to-next balancing of series-connected lithium-ion cells," in *2011 Twenty-Sixth Annual IEEE Applied Power Electronics Conference and Exposition (APEC)*, 2011, vol. 29, no. 9, pp. 1374–1381.
- [41] D. Lewis, "Bidirectional current pump for battery charge balancing," US5631534, 1997.
- [42] N. H. Kutkut and D. M. Divan, "Dynamic equalization techniques for series battery stacks," in *International Telecommunications Energy Conference*, 1996, pp. 514–521.
- [43] J. Moran, "PowerPump™ Balancing," 2011.
- [44] R. H. Park, "Method of equalizing the voltages of the individual cells of storage batteries," US4331911, 1982.
- [45] H. L. W. Deepakraj M. Divan, Nasser H. Kutkut, Donald W. Novotny, "Battery charging using a transformer with a single primary winding and plural secondary windings.pdf," 5659237, 1997.
- [46] N. H. Kutkut, D. M. Divan, and D. W. Novotny, "Charge Equalization for Series Connected Battery Strings," *IEEE Trans. Ind. Appl.*, vol. 31, no. 3, pp. 562–568, 1995.
- [47] N. H. Kutkut, H. L. N. Wiegman, D. M. Divan, and D. W. Novotny, "Design considerations for charge equalization of an electric vehicle battery system," *IEEE Trans. Ind. Appl.*, vol. 35, no. 1, pp. 28–35, 1999.
- [48] N. H. Kutkut, H. L. N. Wiegman, D. M. Divan, and D. W. Novotny, "Design considerations for charge equalization of an electric vehicle battery system," in *Proceedings of 1995 IEEE Applied Power Electronics Conference and Exposition – APEC'95*, 1995, vol. 35, no. 1, pp. 96–103.
- [49] M. Daowd, N. Omar, P. van den Bossche, and J. van Mierlo, "A review of passive and

- active battery balancing based on MATLAB/Simulink,” *Int. Rev. Electr. Eng.*, vol. 6, no. 7, pp. 2974–2989, 2011.
- [50] F. Baronti, G. Fantechi, R. Roncella, and R. Saletti, “High-efficiency digitally controlled charge equalizer for series-connected cells based on switching converter and super-capacitor,” *IEEE Trans. Ind. Informatics*, vol. 9, no. 2, pp. 1139–1147, 2013.
- [51] T. H. Phung, A. Collet, and J. C. Crebier, “An optimized topology for next-to-next balancing of series-connected lithium-ion cells,” *IEEE Trans. Power Electron.*, vol. 29, no. 9, pp. 4603–4613, 2014.
- [52] M. Uno and A. Kukita, “Single-Switch Single-Transformer Cell Voltage Equalizer Based on Forward-Flyback Resonant Inverter and Voltage Multiplier for Series-Connected Energy Storage Cells,” *IEEE Trans. Veh. Technol.*, vol. 63, no. 9, pp. 4232–4247, Nov. 2014.
- [53] A. M. Imtiaz and F. H. Khan, “Time shared flyback converter’ based regenerative cell balancing technique for series connected li-ion battery strings,” *IEEE Trans. Power Electron.*, vol. 28, no. 12, pp. 5960–5975, 2013.
- [54] B. T. Kuhn, G. E. Pitel, and P. T. Krein, “Electrical properties and equalization of lithium-ion cells in automotive applications,” in *2005 IEEE Vehicle Power and Propulsion Conference, VPPC, 2005*, vol. 2005, pp. 55–59.
- [55] Samsung, “INR18650-35E.” Samsung SDI, 2015.
- [56] H. S. Park, C. E. Kim, G. W. Moon, J. H. Lee, and J. K. Oh, “Two-stage cell balancing scheme for hybrid electric vehicle lithium-ion battery strings,” in *PESC Record – IEEE Annual Power Electronics Specialists Conference, 2007*, pp. 273–279.
- [57] C. H. Kim, M. Y. Kim, H. S. Park, and G. W. Moon, “A modularized two-stage charge equalizer with cell selection switches for series-connected lithium-ion battery string in an HEV,” *IEEE Trans. Power Electron.*, vol. 27, no. 8, pp. 3764–3774, 2012.
- [58] Hong-Sun Park, Chol-Ho Kim, Ki-Bum Park, Gun-Woo Moon, and Joong-Hui Lee, “Design of a Charge Equalizer Based on Battery Modularization,” *IEEE Trans. Veh. Technol.*, vol. 58, no. 7, pp. 3216–3223, Sep. 2009.
- [59] H. S. Park, C. H. Kim, and G. W. Moon, “Charge equalizer design method based on battery modularization,” in *2008 IEEE International Conference on Sustainable Energy Technologies, ICSET 2008, 2008*, pp. 558–563.
- [60] “(No Title).” [Online]. Available: <https://shop.gwl.eu/docs/pdf/Winston-OperatorManual.pdf>. [Accessed: 17-Dec-2020].
- [61] “Shenzhen Smart Lion Power Battery Limited.” [Online]. Available: http://en.winston-battery.com/index.php/products/power-battery/item/wb-lyp40aha?category_id=182. [Accessed: 10-Dec-2020].
- [62] C. H. Kim, M. Y. Kim, and G. W. Moon, “A modularized charge equalizer using a battery monitoring ic for series-connected li-ion battery strings in electric vehicles,” *IEEE Trans. Power Electron.*, vol. 28, no. 8, pp. 3779–3787, 2013.



Kristaps Vītols was born in 1986 in Valmiera. He received a Bachelor's degree in Electrical Engineering in 2008 and a Master's degree in 2010 from Riga Technical University. He has worked in the Institute of Industrial Electronics and Electrical Engineering of Riga Technical University since 2008 and currently is a researcher and laboratory manager. His research interests include power electronics, batteries and their related technologies.